



TAMPEREEN TEKNILLINEN YLIOPISTO
TAMPERE UNIVERSITY OF TECHNOLOGY

MARIANNE WUORELA
LED STIMULATION SETUP FOR RETINAL RECORDINGS
Master of Science Thesis

Examiners: Professor Jari Hyttinen,
Post-doctoral researcher Soile
Nymark
Examiners and topic approved in the
Computing and Electrical
Engineering Faculty Council
meeting on 6 February 2013.

ABSTRACT

TAMPERE UNIVERSITY OF TECHNOLOGY

Degree Programme in Electrical Engineering

WUORELA, MARIANNE: LED stimulation setup for retinal recordings

Master of Science Thesis, 46 pages, 1 Appendix page

June 2013

Major subject: Biomedical Engineering

Examiners: Professor Jari Hyttinen, Post-doctoral researcher Soile Nymark

Keywords: retina, electroretinogram, microelectrode array, light-emitting diode, age-related macular degeneration

Retinal degenerative diseases such as glaucoma and age-related macular degeneration are one of the leading causes of blindness worldwide. Currently, there are a limited amount of treatment methods for these diseases. Therefore, many studies conducted in the field of vision research examine the functioning of the retina and try to find possible treatment methods for different retinal degenerative diseases.

The most common way of studying the functioning of retinal cells is to record an electroretinogram (ERG). ERG is a light-evoked extracellular field potential that sums up the activity of retinal cells. Different wave components of ERG can be attributed to specific cell layers, thus enabling tracking of the origin of possible abnormalities in the ERG. ERG can be recorded both from humans and animals, and in vision research, mice and rats are popular animal models because of their genetic manipulations. Their retinas also correspond well with the human peripheral retina and their photoreceptors are quite similar to human photoreceptors.

The retina is typically stimulated by light in vision research. The objective of this thesis is to construct a reliable light stimulation setup for retinal recordings of isolated mouse retinas. This thesis designs, constructs, and tests such stimulation setup. In the literature part of the thesis, the theory related to the functioning of the eye as well as the working principle of the ERG is discussed. In the research part, the stimulation setup is designed and constructed. As a result, the functioning of the setup is tested.

The light source of the stimuli is a light-emitting diode (LED) that has a wavelength of 505 nm in order to cover the peak absorption wavelengths of the mouse retina. The LED has to be able to produce stimulus pulses with adjustable intensities, durations, forms, and frequencies. The LED is controlled via a stimulus generator and an LED controller. The light beam is guided from the LED to the retinal sample with a liquid light guide. Furthermore, the light beam is homogenized and gathered with diffuser and condenser lenses and its intensity is decreased with neutral density filters. The recording of the ERG is done with a microelectrode array (MEA) that is placed inside a Faraday cage. The retinal sample is placed on the MEA plate and kept alive with continuous perfusion.

The setup was tested in order to evaluate its functionality. The testing was done by calibrating the light output and by recording ERGs from isolated mouse retina. The light calibration results showed linear intensity behaviour and an ability to produce different waveforms. The ERG recordings showed typical waveforms. The setup met the requirements and it can therefore be regarded as successful.

TIIVISTELMÄ

TAMPEREEN TEKNILLINEN YLIOPISTO

Sähkötekniikan koulutusohjelma

WUORELA, MARIANNE: LED-pohjainen stimulussysteemi verkkokalvon sähköisiin mittauksiin

Diplomityö, 46 sivua, 1 liitesivu

Kesäkuu 2013

Pääaine: Lääketieteellinen tekniikka

Tarkastajat: professori Jari Hyttinen, tutkijatohtori Soile Nymark

Avainsanat: verkkokalvo, elektroretinogrammi, mikroelektrodimatriisi, hohtodiodi, silmänpohjan ikärappeuma

Verkkokalvon neurodegeneratiiviset sairaudet, kuten glaukooma ja silmänpohjan ikärappeuma ovat maailmanlaajuisesti yleisimpiä sokeuden aiheuttajia. Tällä hetkellä näihin sairauksiin ei ole riittävästi hoitomenetelmiä. Tämän vuoksi monet silmätutkimuksen alalla tehtävät tutkimukset tarkastelevat verkkokalvon toimintaa ja yrittävät löytää hoitomenetelmiä erilaisiin verkkokalvon neurodegeneratiivisiin sairauksiin.

Yleisin tapa tutkia verkkokalvon solujen toimintaa on rekisteröidä elektroretinogrammi (ERG). ERG on valostimulaation aiheuttama ekstrasellulaarinen kenttäpotentiaali, joka muodostuu verkkokalvon solujen sähköisestä aktiivisuudesta. ERG:n aaltokomponentit ovat verkkokalvon eri solukerrostien aiheuttamia, minkä vuoksi mahdollisen epänormaalin aaltomuodon aiheuttajan löytäminen on mahdollista. ERG voidaan rekisteröidä niin ihmisestä kuin eläimestäkin. Näköaistiin liittyvissä tutkimuksissa käytetään yleisesti eläinmalleina hiiriä ja rottia niiden geneettisen manipulaation tarjoamien mahdollisuuksien takia. Niiden verkkokalvot myös vastaavat läheisesti ihmisen verkkokalvon reunaosia, ja niiden näköaistinsolut ovat hyvin samankaltaisia ihmisen näköaistinsolujen kanssa.

Näköaistia tutkittaessa verkkokalvoa stimuloidaan tyypillisesti valolla. Tämän diplomityön tavoitteena on rakentaa luotettava valostimulussysteemi verkkokalvon sähköisiin mittauksiin hiiren eristetyistä verkkokalvoista. Diplomityössä suunnitellaan, rakennetaan ja testataan tällainen stimulussysteemi. Työn kirjallisuusosiossa käsitellään silmän toimintaan ja ERG:n toimintaperiaatteeseen liittyvää teoriaa. Tutkimusosiossa stimulussysteemi suunnitellaan ja rakennetaan, ja tulososiossa sen toiminta testataan.

Stimuloinnin valonlähteenä käytetään hohtodiodia (ledi), jonka aallonpituudeksi valittiin 505 nm hiiren verkkokalvon absorptiomaksimien aallonpituuksien perusteella. Hohtodiodin tulee tuottaa stimuluspulsseja, joiden intensiteettiä, kestoja, aaltomuotoa ja välähdystaajuutta voidaan säätää. Hohtodiodin ohjaamiseen käytetään pulssigeneraattoria ja hohtodiodiohjainta. Ennen kuin valokeila ohjataan hohtodiodilta verkkokalvolle valokuidun avulla, se homogenisoidaan ja kootaan linssien avulla ja sen intensiteettiä lasketaan neutraalien harmaasuotimien avulla. ERG:n rekisteröinti tehdään Faradayn häkin sisälle asetetun mikroelektrodimatriisin avulla. Eristetty verkkokalvo asetetaan elektrodimatriisin päälle, missä se pidetään hengissä perfuusion avulla.

Stimulointisysteemi testattiin sen toiminnallisuuden varmistamiseksi kalibroimalla valostimulukset ja rekisteröimällä hiiren verkkokalvon ERG. Kalibraatiotulokset osoittivat intensiteetin käyttäytyvän lineaarisesti sekä sen, että stimuluksia voidaan tuottaa eri aaltomuodoissa. ERG-rekisteröinneistä saatiin tyypillisiä käyrämuotoja. Stimulointisysteemi vastaa asetettuja vaatimuksia ja työtä voidaan pitää onnistuneena.

PREFACE

This Master of Science thesis was done at and funded by the Department of Electronics and Communications Engineering of Tampere University of Technology. The setup was constructed and tested at the Regea Cell and Tissue Center.

I wish to express my gratitude to my supervisor Professor Jari Hyttinen for giving me the opportunity to work on this project. His advice and support were invaluable. I also want to thank my supervisor Post-doctoral researcher Soile Nymark for her constant support, advice, and kindness.

I want to thank my family for the love and support that I have received throughout my studies. I am forever grateful to my daughter Minea and my fiancé Daniel without whom I could not have done this.

Tampere 14.5.2013

Marianne Wuorela

CONTENTS

1	INTRODUCTION	1
2	THEORETICAL BACKGROUND	3
2.1	The Eye and the Retina	3
2.1.1	Photoreceptors	5
2.1.2	Ganglion Cells	6
2.1.3	Retinal Pigment Epithelium.....	6
2.2	Retinal Electrophysiology	8
2.2.1	Phototransduction	8
2.2.2	Visual Signal Processing	9
2.2.3	Photoreceptor responses	10
2.3	Electroretinogram.....	12
2.3.1	Measurement	13
2.3.2	Waveform	13
2.3.3	ERGs of Isolated Retinas.....	14
2.3.4	Light Stimulus	16
3	RESEARCH METHODS AND MATERIALS	19
3.1	Parameter Requirements	19
3.2	Measurement Setup	20
3.3	Light Stimulation Setup	22
3.4	Measurement	24
3.4.1	Calibration	25
3.4.2	Tissue preparation.....	25
3.4.3	MicroERG Recording.....	26
4	RESULTS	28
4.1	Construction of the Setup.....	28
4.2	Light calibration	31
4.3	Measurements with Retinal Samples	34
5	DISCUSSION	38
5.1	The Setup	38
5.2	The Stimulator Output.....	39
5.3	The MicroERGs	40
6	CONCLUSIONS.....	41
	REFERENCES.....	42
	APPENDIX 1: MEASURED RADIANT POWER VALUES AND CALCULATED INTENSITY VALUES	47

NOTATIONS AND ABBREVIATIONS

A	Area
c	Speed of light
d	Optical density
E	Energy
f	Frequency
h	Planck's constant
I	Intensity
λ	Wavelength
P	Power
r	Radius
A/D	Analog-to-digital
AMD	Age-related macular degeneration
BRB	Blood-retinal barrier
bv	Blood vessel
cGMP	Cyclic-guanosine monophosphate
ERG	Electroretinogram
GCL	Ganglion cell layer
iGluR	Ionotropic glutamate receptor
ILM	Inner limiting membrane
INL	Inner nuclear layer
IPL	Inner plexiform layer
IPM	Interphotoreceptor matrix
LED	Light-emitting diode
MEA	Microelectrode array
mGluR	Metabotropic glutamate receptor
MicroERG	Microelectroretinogram
ND	Neutral density
OLM	Outer limiting membrane
ONL	Outer nuclear layer
OPL	Outer plexiform layer
PDE	Phosphodiesterase
pMEA	Perforated microelectrode array
RPE	Retinal pigment epithelium

1 INTRODUCTION

The ‘Global data on visual impairments 2010’ study conducted by the World Health Organization states that in 2010 there were around 285 million visually impaired and 39 million blind people worldwide. The leading causes of blindness are cataract (51%), glaucoma (8%), and age-related macular degeneration (AMD) (5%). Successful treatment methods such as surgery exist for cataract and glaucoma. For AMD, there are only a limited amount of treatment methods available. (World Health Organization 2010; World Health Organization 2013)

In industrialized countries, AMD is the primary cause of blindness. It affects the macula of the eye, thus causing loss of sight in the center of the vision leaving only the peripheral vision functional. AMD has two forms: dry and wet. In the dry form, the retinal pigment epithelium (RPE) gets thinner and degenerates over time as a consequence of extracellular material build-up in the RPE and the retina. The death of the RPE leads to the loss of photoreceptors in the retina thus causing blindness. In the wet form there is an abnormal growth of new blood vessels that leak fluids and blood into the RPE and the retina. This compromises the blood-retinal barrier (BRB) that protects the delicate retina. As a consequence, the detachment of the RPE from the retina and ultimately the damage of the retina will follow. (International Macular Degeneration; World Health Organization 2013)

The role of the BRB and the RPE in protection and maintenance of the retina has been studied extensively. Several studies have been conducted in order to study the functioning of the BRB and the RPE-photoreceptor interface (Cunha-Vaz 2004; Strauss 2005; Wimmers et al. 2007). Electroretinograms (ERGs) measure the electrical behaviour of retinal cells and it is an important method in studying the functioning of different retinal cells. Animal models, such as mice and rats, are widely used for ERG recordings as they provide an approximation to human responses (Ekesten et al. 1998; Peachey et al. 2003; Robson et al. 2004; Pinto et al. 2007; Heikkinen et al. 2008). Both mice and rats have naturally occurring mutants, but they can also be genetically manipulated and thus different retinal degenerations can be induced (Vinores et al. 2000; Chang et al. 2002; Rakoczy et al. 2006). This enables the studies of different retinal diseases and the discovery of possible treatment methods (Binder et al. 2007; Gerth 2009; Bhutto & Luty 2012).

The objective of this thesis is to design, construct, and test a light stimulation setup for vision research. The setup is used in *in vitro* ERG recordings that provide essential information of the functioning of the cells. This information is utilized in different vision research studies, such as the study of retinal degenerative diseases.

The stimulation setup is used in the Development of an in Vitro Measuring System for Ophthalmic Applications project led by Academy of Finland Post-doctoral researcher Soile Nymark. The project is part of the collaboration between the research group led by Professor Jari Hyttinen and the Ophthalmology group led by Academy of Finland Research Fellow Heli Skottman, and belongs to a larger collaboration project, Human Spare Parts, funded by the Finnish Funding Agency for Technology and Innovation. The stimulation setup is located at the Regea Cell and Tissue Center.

Similar kinds of setups have been used in different ophthalmic studies. For example, Tian & Copenhagen (2003) and Herrmann et al. (2008) studied ganglion cell responses of mouse retinas and ERGs of rat retinas, respectively. Both studies used light-emitting diodes (LEDs) for stimulation and 60-channel microelectrode arrays (MEAs) for recording. The LED peak wavelengths were 567 nm for Tian & Copenhagen and 505 nm for Herrmann et al. The wavelength depends on the animals used in the study.

In this thesis, the constructed setup utilizes the 60-channel MEA as well. The stimulation is done with an LED that has a peak wavelength of 505 nm. The LED choice is based on the use of mice as animal models. Thus, the setup is very similar to the ones presented above. However, the articles do not state how the stimulus is delivered to the retina thus preventing a more profound comparison between them and the setup constructed here.

The development process of the stimulation setup started with background research. The theory relevant to the thesis topic is discussed in the theoretical part of the thesis. The basic anatomical and physiological aspects of the retina as well as the measurement of the ERG and its basic features are examined.

In the practical part of the thesis, the developed stimulation setup is introduced. The setup design started with listing the required parameters. The components were chosen according to these parameters and the setup was constructed. The constructed setup was tested and its functionality was evaluated in two parts. First, the light stimuli were calibrated by measuring the power and intensity values with different input voltages. In addition, the ability to produce stimulus pulses with adjustable intensities, forms, durations, and frequencies was tested. In the second part, the setup was tested by recording ERGs from isolated mouse retina.

2 THEORETICAL BACKGROUND

The basic anatomy of the human eye as well as the most important cell structures relevant to the thesis topic are discussed in this chapter. The electrophysiological responses of the retina are examined and the theory behind the electroretinogram (ERG) is discussed.

2.1 The Eye and the Retina

The retina is a thin membrane located in the bottom of the eye. As a part of the central nervous system, the retina is a very delicate structure. It is easily accessible and thus it can be studied without any major obstacles. The retina converts absorbed photons into a train of electrical pulses. The pulses travel through the optic nerve to the visual cortex of the brain. The brain interprets these pulses as the picture that the eyes saw. Figure 2.1 illustrates the structure of the human eye and the location of the retina. (Webvision 2011.)

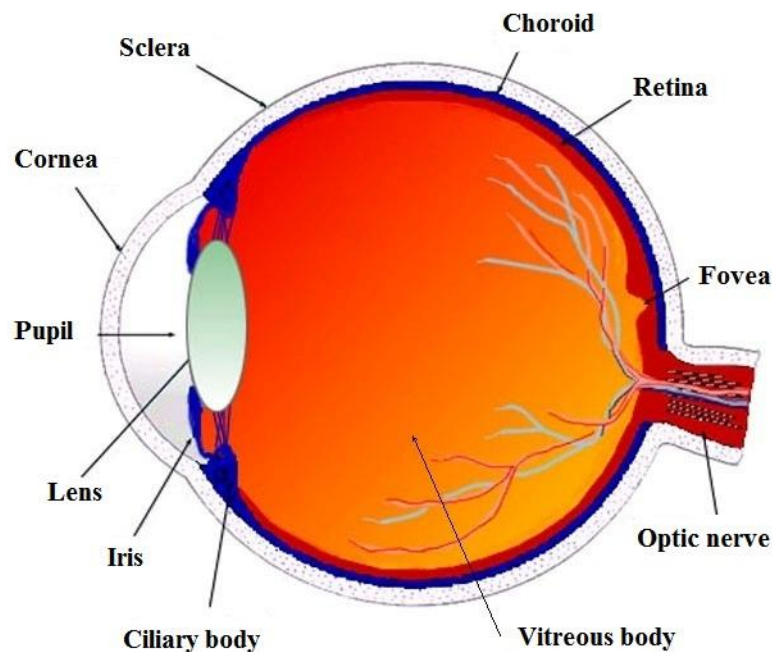


Figure 2.1. The structure of the human eye (modified from Webvision 2011).

As can be seen in Figure 2.1, the retina is located between the vitreous body and the choroid. Photon-absorbing photoreceptors, rods and cones, are located in the outermost layer of the retina and the ganglion cells that send the visual signals to the brain are

located in the innermost layer of the retina. The optic disc is the area where the optic nerve passes through the retina. In this area, there are no photoreceptors, therefore the optic disc is also called the blind spot. In the human eye, the fovea is located on the left side of the optic disc, in the middle of macula. The fovea is responsible for the sharp central vision. In the fovea area, all the other cellular structures of the retina are pushed to the sides so that there is only a thin layer of cone cells. (Wandell 1995.)

The retina is a layered structure of neural cells and can be divided into three layers of nerve cell bodies and two layers of synapses. In Figure 2.2, the layers are presented so that another tissue layer, the retinal pigment epithelium (RPE), is on top. Right under the pigment epithelium there are the outer segments of the photoreceptors under which there is the outer nuclear layer (ONL) that contains the cell bodies of the rods and cones. The inner nuclear layer (INL) contains the cell bodies of the amacrine, horizontal, and bipolar cells. The synapse layer between the ONL and the INL is called the outer plexiform layer (OPL). The rods and cones connect with the horizontal and bipolar cells in the OPL. The innermost layer of the cell bodies is called the ganglion cell layer (GCL). It contains not only the cell bodies of the ganglion cells but also some displaced amacrine cells. The synapse layer between the INL and the GCL is called the inner plexiform layer (IPL). The ganglion cells connect with the bipolar cells in this layer. However, it is known that also amacrine cells influence the signal processing in ganglion cells. The IPL is an important processing layer of the visual signal on the way to the brain. (Wandell 1995; Kolb 2006)

In addition to the structure introduced above, two other layers are considered as part of the retinal structure: the outer limiting membrane (OLM) and the inner limiting membrane (ILM). The OLM is a layer where the photoreceptors and Müller cells connect. It is located between the ONL and the outer segments of the rods and cones. Müller cells are glial cells that spread almost throughout the entire width of the retina. The cells run radially from the ILM to the OLM. It is believed that the functions of the Müller cells are the maintenance of potassium levels in the retina, participation in the retinal carbohydrate metabolism, participation in the cone visual cycle (Wang & Kefalov 2011), and partial control of the composition of the interphotoreceptor matrix. The ILM is a similar kind of structure between the ends of the Müller cells and the basement membrane constituents. The ILM functions as a barrier between the vitreous humor and the neural retina. The OLM also functions as a barrier between the RPE and the neural retina. (Wandell 1995; Hageman & Johnson 2006).

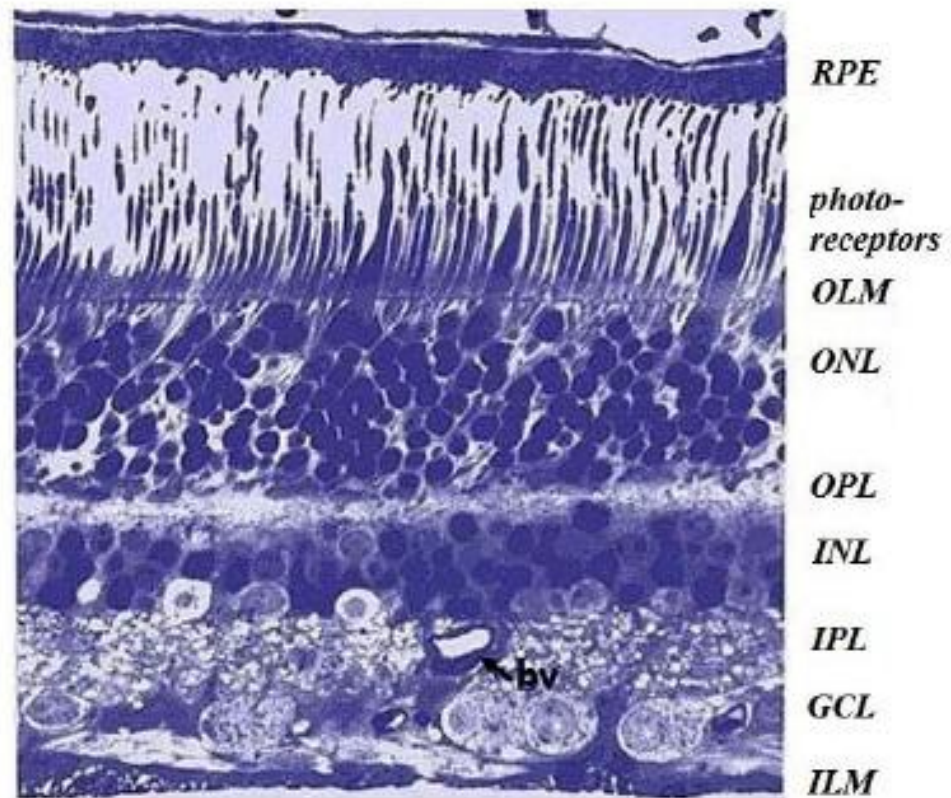


Figure 2.2. Light microscopic image of the retinal structure (modified from Webvision 2011).

The neural tissue of the retina is supplied with blood by the choriocapillaries running from the GCL to the OPL, sometimes even to the ONL. Choriocapillaries of this kind can be seen in Figure 2.2 marked as 'bv' (blood vessel). The photoreceptors on the other hand are supplied by the choriocapillaries running behind the RPE. (Webvision 2011.)

2.1.1 Photoreceptors

Photoreceptors are light sensing neurons that convert photons into electrical signals in the retina. They are located in the bottom of the eye right below the RPE. There are two types of photoreceptors: rods and cones. The rod cells outnumber the cones with around 100 million as there are only around five million cone cells in the human retina. The concentrations of both photoreceptors vary across the retina. However, there are only cone cells in the fovea. (Wandell 1995.)

Both rod and cone cells contain visual pigment that is located in the disk membranes of the outer segments of the cells (Gross & Wensel 2011). Visual pigment consists of the retinal-bound opsin. In rod cells, there is only one type of opsins whereas in cone cells there are three different types of opsins. Depending on the opsin structure, cone cells are divided into three wavelength categories: short, medium, and long

wavelengths. Short wavelength cone cells are most sensitive to blue light with an absorption maximum at 430 nm to 440 nm. Medium wavelength cone cells are most sensitive to green light with an absorption maximum at 530 nm whereas long wavelength cone cells are most sensitive to red light with an absorption maximum at 560 nm to 570 nm. Rod cells on the other hand are most sensitive to blue-green light and they have their absorption maximum at 500 nm. Rod cells are responsible for the visual perception in dim and dark conditions, whereas cone cells are responsible for the perception of colors and for the visual perception in bright light conditions. (Wandell 1995.)

2.1.2 Ganglion Cells

Ganglion cells function as the output of the visual signal. Visual stimuli from photoreceptors are conveyed to ganglion cells by bipolar and amacrine cells. Ganglion cells convert these stimuli into action potentials before conveying them to the brain through the optic nerve that consists of their axons. (Kolb 2006.)

There are several subtypes of ganglion cells. Different subtypes respond to illumination in a sustained or transient fashion and transmit information about the form, color, motion, and spatial relationship. One type of cells respond to image motion in specific directions. (Marc 2011.)

Ganglion cells receive their inputs from those photoreceptors that form their receptive fields. The receptive fields are circular in shape and they have center and surround regions. ON center cells are stimulated when light hits the center and inhibited when light stimulates the surrounding. For the OFF center cells, the opposite principle applies. This type of difference in the light intensity between the center and surround enables the detection of contrast. (Rodieck 1998.)

Ganglion cells convey the visual signals from photoreceptors in parallel ON center and OFF center pathways. The pathways carry different kinds of information of the detected image. One pathway (cell type P) carries the information of fine detail whereas the other pathway (cell type M) carries the information of larger, fast action images. (Kolb 2006; Lukasiewicz & Eggers 2011)

2.1.3 Retinal Pigment Epithelium

Retinal pigment epithelium is a monolayer of pigmented cells that have tight junctions between them. RPE is adjacent to the photoreceptors and the interphotoreceptor space that is between the apical side of the RPE and the outer segments of the photoreceptors is filled with the interphotoreceptor matrix (IPM). The IPM forms the RPE-photoreceptor interface, thus being essential for the interactions between the RPE and photoreceptors. For example, the IPM mediates biochemical interactions between the choroid, RPE, and retina. On the basolateral side, RPE is attached to Bruch's membrane. Bruch's membrane is part of the extracellular matrix that separates the RPE from the capillaries of the choroid (choriocapillaries). It forms the interface between the

RPE and the choroid. Together the RPE, Bruch's membrane and the endothelium of the choriocapillaries form the outer blood-retinal barrier (BRB). The inner BRB consists of the retinal capillaries that run inside the eye and supply the inner layer of the retina. The BRB as a whole plays an important role in the health and disease of the retina in terms of regulation of transportation processes. (Cunha-Vaz 2004; Hageman & Johnson 2006; Wimmers et al. 2007)

The RPE-photoreceptor interface is of crucial importance to the retinal wellbeing. It performs various functions in terms of maintenance of retinal cell function and homeostasis. For example, the RPE cells phagocytose the fragments of the photoreceptor outer segments during photoreceptor renewal. RPE also absorbs the excess light in the retina that is not absorbed by the photoreceptors. In addition, RPE has other functions such as the transportation of substances through the interface, maintenance of ionic balance around the photoreceptors, participation in the visual cycle to retain photoreceptors' light sensing ability, secretion of different substances, and supporting the immune privilege of the inner eye. Figure 2.3 illustrates the structure of the photoreceptors, RPE, Bruch's membrane, and choriocapillaries. (Strauss 2005; Hageman & Johnson 2006)

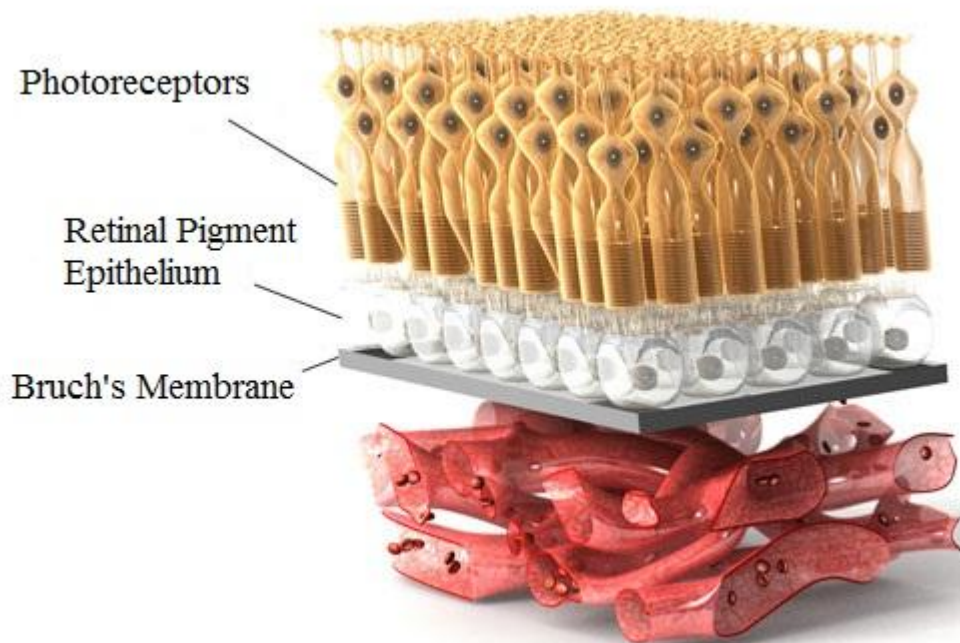


Figure 2.3. Schematic of the structure of the photoreceptors, retinal pigment epithelium, Bruch's membrane, and choriocapillaries (modified from *The Angiogenesis Foundation* 2013).

Alteration of the BRB is believed to be the cause of the age-related macular degeneration (AMD) (Binder et al. 2007). Due to its wide global distribution and lack of treatment methods, AMD has become a popular topic in ophthalmic research. Vinore

et al. (2000) studied the breakdown of the BRB and its role in the development of the AMD. The use of RPE transplants as a potential treatment method has been studied by Binder et al. (2007) and da Cruz et al. (2007), for example. These studies discuss different aspects of the use of RPE transplants in retardation and restoring of visual loss.

2.2 Retinal Electrophysiology

Visual signals are processed in the complex neuronal network of the retina before the post-retinal signal processing of the brain. The process starts from the phototransduction in the photoreceptor layer and continues through various pathways. The final processing of the signal occurs in the ganglion cell layer before the signal is passed through to the optic nerve to be further processed by the brain.

2.2.1 Phototransduction

Phototransduction is a process by which photons are converted into electrical signals in photoreceptors. Phototransduction is quite similar in both rods and cones, so the overall picture of this process presented here is only for rods. Anatomically, both rods and cones consist of an inner and outer segment, a cell body and a synaptic region. Through the synaptic region, the photoreceptor cell passes a chemical signal to the second order retinal nerve cell. The following retinal nerve cells then pass the signal to the brain. (Alberts et al. 2008.)

The outer segment of the rod photoreceptor consists of discs that are stacked on top of each other. Each disc contains visual pigment molecules called rhodopsin. The outer segment is surrounded by a plasma membrane that contains cyclic-guanosine monophosphate (cGMP)-gated cation channels. The cGMP is a cyclic nucleotide that acts as a second messenger. The cGMP-gated channels stay open in the dark when cGMP is bound to them. When the channels are open, there is an inward current of Na^+ ('dark current') and an outward current of K^+ . The cell is depolarized and neurotransmitters are being released from the synaptic region. (Alberts et al. 2008.)

The process of phototransduction occurs via a G-protein-coupled pathway. The G-protein-coupled receptor is opsin that contains chromophore 11-*cis* retinal. When a photon is absorbed, the 11-*cis* retinal isomerizes into all-*trans* retinal. The photoisomerization changes the conformation of the retinal and this forces a change in the conformation of the opsin. The activated rhodopsin induces a change in the conformation of a G-protein called transducin, which then activates cGMP phosphodiesterase (PDE). The cGMP in the cytoplasm is hydrolyzed by the activated PDE molecules and this makes the cytosolic cGMP concentration fall. The drop in cGMP concentration causes the plasma membrane –bound cGMP molecules to leave their binding sites which leads to the closure of cation channels and hyperpolarization of the cell. During hyperpolarization the rate of neurotransmitter release is reduced in the synapse and the signal is conveyed to other retinal neurons. The light signal is converted

into an electrical one in the photoreceptor when the signal passes from the disc membrane to the plasma membrane. The generated signal travels from the photoreceptor outer segment through the inner segment and cell body into the synaptic region. From there it then travels through the other retinal nerve cells to the brain. Figure 2.4 illustrates the depolarization and hyperpolarization of a rod. (Alberts et al. 2008.)

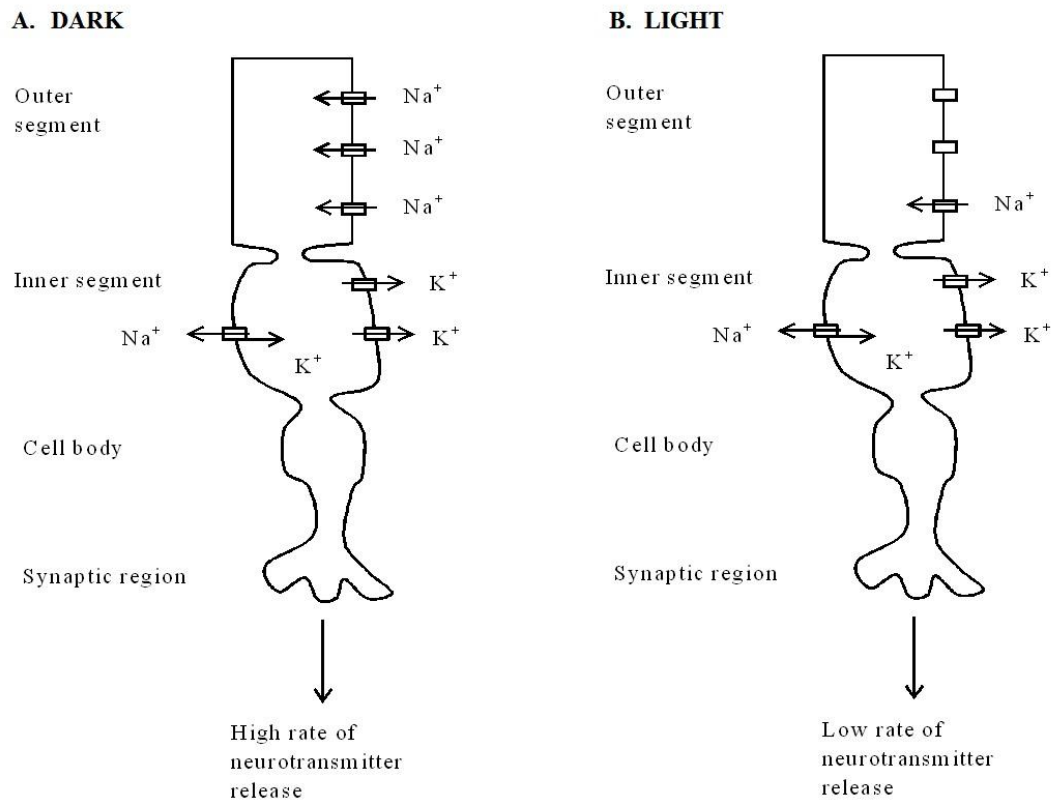


Figure 2.4. Schematic of a rod cell. A) The cell is depolarized in the dark. B) The cell is hyperpolarized via phototransduction. (redrawn from Alberts et al. 2008)

Several negative feedback systems are used when rods return to their resting state or when they need to adapt to continuous illumination. Furthermore, the light sensing chromophore molecules need to be regenerated after the photon absorption in order to keep the rods' ability to be activated by light. This regeneration is performed in the RPE and it is crucial not only for the rods but also for the cones. (Alberts et al. 2008.)

2.2.2 Visual Signal Processing

When light enters the eye it has to travel through the cornea, the aqueous humor, the lens, and the vitreous body (see Figure 2.1) before reaching the retina. Inside the retina, light has to travel through all cell layers in order to reach the photoreceptors. The photoreceptor cells can sense light through the light-absorbing visual pigment. The absorbed photons change the form of the visual pigment resulting in the phototransduction cascade. This cascade generates a change in photoreceptor membrane potential which is the origin of the signal that travels through the other retinal neurons.

When the signal finally reaches the ganglion cells, it is converted into action potentials. The axons of the ganglion cells form the optic nerve through which the signal is conducted into the visual cortex of the brain. (Schor & Miller 2011; Gross & Wensel 2011)

The signal pathway from photoreceptors to ganglion cells can be divided in two pathways, rod pathway and cone pathways, which differ from one another. Rods are very sensitive cells and they respond slowly to feature changes in dim light against dark background. Cones on the other hand detect bright lights and their rapid fluctuations. They respond to such features as edges, bright colors against dark ones or vice versa. (Kolb 2006.)

Rods and cones both synapse with bipolar and horizontal cells. In human retina, rod bipolar cells gather information from 15 to 50 rod cells. This ratio is smaller in cone pathway: around 10-25 cones converge to 1-6 cone bipolar cells. In this synaptic layer, rod and cone signals are separated so that rods synapse with one type of bipolar cells whereas cones synapse with various types of bipolar cells. (Rodieck 1998.)

Bipolar cells can be divided into excitatory and inhibitory types based on their receptors. Excitatory bipolar cells have ionotropic glutamate receptors (iGluRs) and inhibitory bipolar cells have metabotropic glutamate receptors (mGluRs). Together these bipolar cells expressing either iGluRs or mGluRs form parallel signal pathways, called ON and OFF pathways, which detect shadow or highlights. ON pathways detect light-on-dark and OFF pathways detect dark-on-light. Vision is based on this: the contrast of one image against a different background. (Kolb 2006.)

Visual signal is divided into ON and OFF pathways throughout the retina. Therefore, similarly to the bipolar cells, ganglion cells are divided into ON and OFF types. Connections occur between the ON type bipolar and ganglion cells and between the OFF type bipolar and ganglion cells. However, only cone bipolar cells synapse directly with ganglion cells. Rod bipolar cells make the connections through amacrine cells. (Rodieck 1998; Kolb 2006)

Visual signal is also processed in other ways than dividing bipolar and ganglion cells into the ON and OFF types. In this signal processing, amacrine cells and horizontal cells have important roles. Horizontal cells, for example, can inhibit the generation of information on certain signal pathways. Amacrine cells, on the other hand, can modulate and integrate the visual signal that is relayed to the ganglion cells. (Rodieck 1998; Kolb 2006)

2.2.3 Photoreceptor responses

Photoreceptor responses reflect changes in voltage or current across the cell membrane due to light absorption. These responses derive from the phototransduction cascade discussed in Chapter 2.2.1. In darkness, the dark current flows into the outer segments of the photoreceptor. When photons are absorbed, the magnitude of the dark current changes and this change is called the photocurrent. Correspondingly, the change in the

transmembrane potential caused by the change in the photocurrent is called photovoltage. (Rodieck 1998; MacLeish & Makino 2011)

In the human retina, photoisomerization of a single visual pigment molecule in a rod cell causes approximately a 2% decrease in the dark current. This response increases with increasing stimulus light intensity up to a certain intensity value. However, as the number of absorbed photons increases, the number of closed cGMP-gated channels per photon decrease. The maximal response is induced when enough photons are absorbed and all cGMP-gates are closed. (Rodieck 1998; MacLeish & Makino 2011)

Rods and cones differ in terms of photocurrent responses. Firstly, cones respond to light faster than rods: the time to peak of a typical mammalian cone flash response is about 50 ms as opposed to the 200 ms time to peak of a typical mammalian rod response. The duration of the cone response is also generally about four times shorter than the rod response. Secondly, the sensitivity of cones to light is lower compared to rods. Therefore, the amplitude of the response to each photoisomerization is about 20 times smaller in cones than in rods. In addition, the cone response is often biphasic: it undershoots the equilibrium level after the response before reaching it again. (Rodieck 1998; MacLeish & Makino 2011) Figure 2.5 illustrates some of these differences between the photocurrent responses of rods and cones of monkey retinas. Note, however, that the sensitivity difference is not evident due to different stimulus light intensities used for stimulating the rod or the cone.

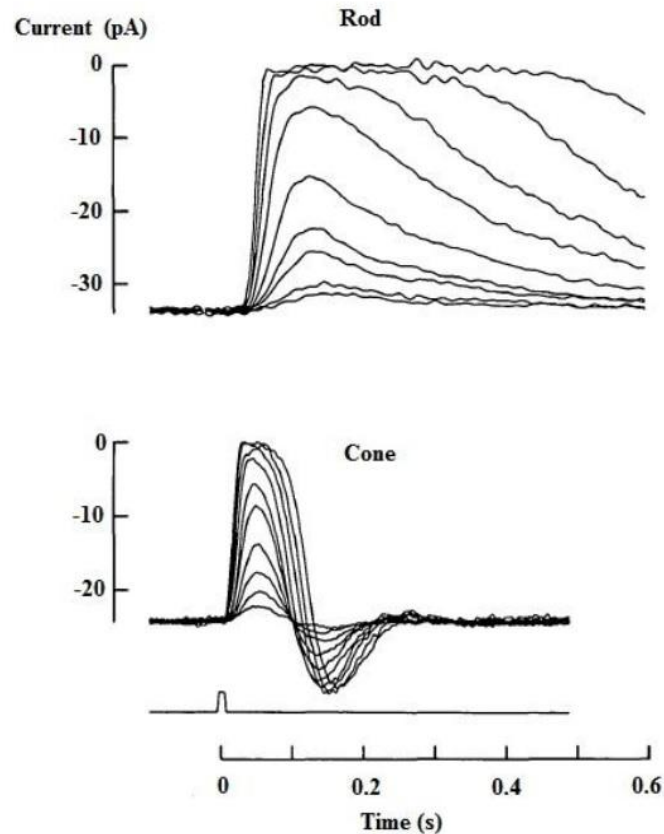


Figure 2.5. The photocurrent responses with different stimulus intensities recorded from a rod cell and a red cone cell of monkey retinas. The given light stimulus pulse is marked below the curves. (modified from Baylor 1987)

In darkness, the approximate value of the transmembrane voltage for both rods and cones is -35 mV. After the absorption of a single photon, the transmembrane voltage hyperpolarizes by about 1 mV in rods. As discussed above, cones are less sensitive thus requiring more photons in order to produce a visible response. However, even though the cone system is not as sensitive as the rod system, it is able to adapt to a wider range of light intensities. (Rodieck 1998; MacLeish & Makino 2011)

2.3 Electroretinogram

Electroretinogram (ERG) is a noninvasive method that can be used to measure light induced potential changes across the eye. These changes arise from the activity of various cell layers of the retina. Therefore, ERG signal is overall a light-evoked extracellular field potential that sums up the activity of the retinal cells. Retinal abnormalities can cause alterations in the ERG waveforms and since different ERG waves can be attributed to specific retinal layers, the value of the ERG as a diagnostic tool is undeniable. (Malmivuo & Plonsey 1995; Guenther et al. 2006)

ERG can also be recorded *in vitro* from an isolated retina. These recordings can be made by using different types of electrodes. The term ‘microERG’ is often attributed to ERG recordings of retinal samples recorded with a microelectrode array (MEA). This technique not only enables the recording of the potential differences across the retina, but also the recording of ganglion cell activity. Since the ganglion cell layer faces the electrodes of the MEA, there is a direct contact between the ganglion cells and the electrodes. In this thesis, the designed setup is for microERG purposes. (Guenther et al. 2006.)

2.3.1 Measurement

In clinical use, ERG is recorded to detect any abnormalities in patient’s retina. In a typical procedure, the measuring electrode is implanted in a contact lens. The contact lens is placed on the patient’s eye while the reference electrode is usually placed on the temple, earlobe or forehead. Bipolar electrodes contain both the measuring and the reference electrode and they are often used for better signal quality and simplicity. Both mono- and bipolar electrode systems also require a ground electrode in order to ground the patient. The ground electrode is placed on the skin away from the reference electrode. The amplitude and polarity of the recorded ERG wave depend on the placement of the recording and ground electrodes. (Frishman 2006; Clark 2010)

During the measurement, the patient is subjected to brief exposures of light that induce the potential changes in the retina. The basic stimulation method is the Ganzfeld globe that induces full-field stimuli. In this method, the background illumination as well as the stimulus intensity can be easily controlled. Typically the measured voltage of the ERG wave ranges from tens of microvolts to a millivolt thus requiring proper amplification. (Malmivuo & Plonsey 1995; Webvision 2011)

MicroERG is recorded with a MEA from a retinal sample, such as a mouse retina. In the measurement, the retina is placed on a MEA plate so that the ganglion cells face the electrodes. The retinal sample is kept alive with continuous perfusion. Similar to the clinical use of the ERG, the retinal sample is subjected to brief exposures of light during the measurement. The induced electrical responses are then recorded with the MEA. (Guenther et al. 2006.)

2.3.2 Waveform

A typical response of human retinal cells to a brief light exposure is a waveform that can be divided into a- and b-waves (Frishman 2006). Often a third wave component, c-wave, can be observed as well. However, the c-wave cannot be detected from an ERG that is recorded from an alert human subject, because the eyes move too frequently for this slow wave (Frishman & Wang 2011). The schematic of a dark-adapted flash ERG wave recorded from a human subject is presented in Figure 2.7.

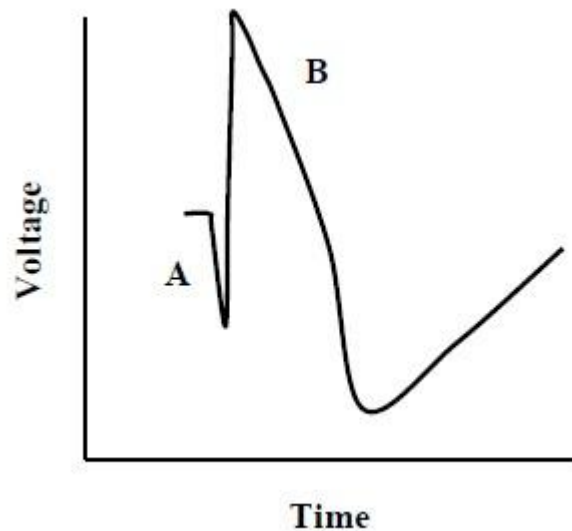


Figure 2.7. Schematic of a dark-adapted flash ERG recorded from a human subject. The basic wave components a and b can be distinguished. (redrawn from Robson & Frishman 1999).

In ERG signal, photoreceptors are the main contributors to the negative a-wave. Both rods and cones contribute to this wave component, so rod- and cone responses can be studied separately only with appropriate stimulus conditions. Under dark-adapted conditions with dim light stimuli, pure rod responses can be recorded. Correspondingly, cone responses can be recorded under light-adapted conditions with brighter light stimuli. (Carr 2006; Frishman 2006)

The positive b-wave in ERG signal is initialized by bipolar cells. Depolarizing ON bipolar cells are the major contributors to this wave component. The remaining positive ERG-wave component, c-wave, is induced by the retinal pigment epithelium as they interact with the rods. The c-wave is very slow in comparison with the b-wave. (Malmivuo & Plonsley 1995; Frishman & Wang 2011)

2.3.3 ERGs of Isolated Retinas

The absence of treatment methods for such retinal diseases as AMD has inspired many studies (Binder et al. 2007; Gerth 2009; Bhutto & Luttly 2012). Different retinal diseases induce the malfunctioning of the retinal cells which can be detected with the recording of the ERGs. Animals are widely used as models for variety of human disorders and ERGs can be recorded from isolated retinas in addition to intact animals. Mice have become popular animal models in the field of ophthalmic research due to the fact that they can be genetically manipulated and are easily bred. By genetic manipulation one can induce different retinal diseases in addition to the naturally occurring genetic mutations. (Naarendorp et al. 2010; Heikkinen et al. 2012)

Mice can be used as human models for several reasons. Mice genomes are proximate to human genomes and the mouse retina serves as a good model for the human peripheral retina. The mouse retina is rod-dominated with a rod concentration of

approximately 97%. The peak sensitivity of the rods is 510 nm. Mouse cones have two peak sensitivities, at 350 nm and 510 nm. The mouse ERG generally has the same wave components as the human ERG, thus facilitating the comparison between the recordings. Figure 2.8 presents a microERG waveform recorded from an isolated rat retina with a MEA. It serves as a good example of a microERG waveform due to the similarity between the mouse and the rat retina. (Nusinowitz & Heckenlively 2006; Naarendorp et al. 2010; Heikkinen et al. 2012)

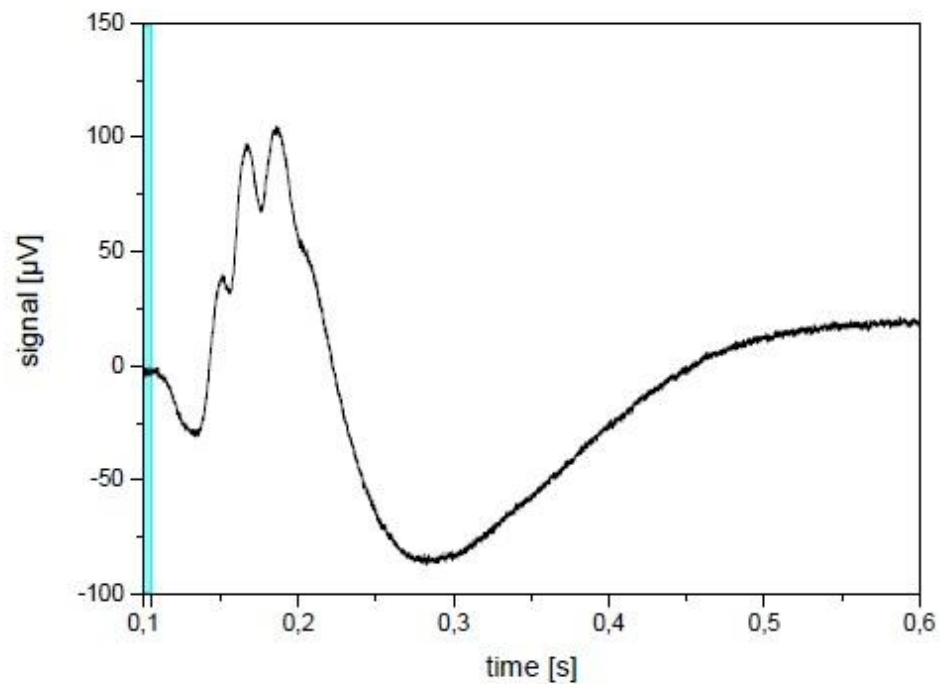


Figure 2.8. *MicroERG waveform of an isolated rat retina (Herrmann et al. 2008).*

As discussed above, retinal recordings with a MEA also reveal ganglion cell responses. An example of ganglion cell action potentials is presented in Figure 2.9. The recording is obtained from a rat retina with a MEA of 61 electrodes.

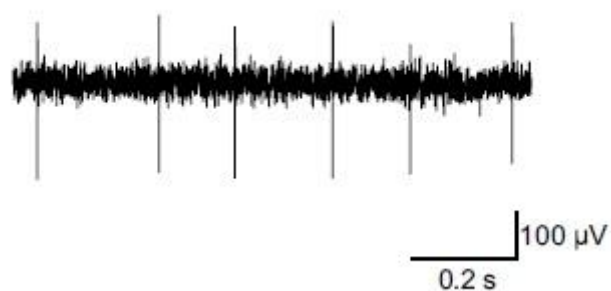


Figure 2.9. *Ganglion cell activity from an isolated rat retina (modified from Sekirnjak et al. 2009).*

Heikkinen et al. (2012) studied the mouse rod responses both from intact animals (*in vivo*) and isolated retinas (*ex vivo*). They compared the gain and kinetics of the ERGs and were able to conclude that the a-waves of the ERGs were similar in terms of size, sensitivity, and kinetics. The b-wave, however, was delayed in the isolated retinas. The most obvious difference between the ERGs was the lack of c-wave in the isolated retinas. This is due to the absence of RPE since the c-wave originates from the RPE. As a conclusion Heikkinen et al. were able to state that the ERGs from isolated retinas and intact animals correspond well with each other, thus justifying the use of isolated retinas in ERG recordings.

Numerous studies have investigated mouse ERGs (Peachey & Ball 2003; Pinto et al. 2007) and especially the responses of the rods and cones (Ekesten et al. 1998; Robson et al. 2004; Heikkinen et al. 2008) and ganglion cells (Tian & Copenhagen 2003). These studies have provided ERGs of healthy animals for example. The recordings are essential in order to understand different retinal diseases and their mechanisms.

Animal models with natural and induced genetic mutations have been reviewed in the articles written by Chang et al. (2002) and Rakoczy et al. (2006). Chang et al. listed sixteen naturally occurring mouse mutants and their geno- and phenotypes. Some comparative data between normal mice and mice with retinal degenerations was provided.

Rakoczy et al. on the other hand examine mouse models of the AMD and listed several transgenic models. Some discussion about using mice as human AMD models was included in the article.

2.3.4 Light Stimulus

Light source and the whole stimulus system play a crucial role in the ERG setup. There are several parameters that have to be taken into account when choosing the stimulus system: intensity, wavelength, size, and duration of the light stimulus as well as the type of the light source. The parameters are defined based on the subject (human or animal) and the questions investigated.

The stimulus can be produced with different light sources such as laser, light-emitting diode (LED), monochromator, or xenon lamp. For isolated retina recordings, the use of LED as a light source is becoming more and more popular due to their easy controllability and availability in various wavelengths and them having quite a large power range. In this chapter, the definition of each stimulus system parameter is discussed while assuming the use of LED as the light source.

Intensity

ERG recordings require a light source that is adjustable in terms of intensity. For example, the mouse retina requires a wavelength of 510 nm to cover both the rods and one type of cones. In order to examine dark-adapted rod response, a logarithmic scale of

approximately 2,5 decades is required for the intensity adjustment. This is due to the fact that rods can detect single photons but they saturate at a level of approximately 500 photons per rod per second. Cones on the other hand, have a much wider intensity scale and this has to be taken into account with the intensity adjustment. Cones require a logarithmic scale of approximately 3,5-4,5 decades, thus making the total intensity range 6-7 decades for the rods and cones. Both rods and cones can, however, change their dynamic range by adapting to ambient illumination thus enabling the human vision to function over an intensity range of 10 decades. (Rodieck 1998.)

The intensity of the light beam varies throughout the beam. Factors such as the shape of the beam, location of the examined spot within the beam, and distance between the light source and the target affect the intensity of the light beam. The beam can take different shapes, but often the beam is not homogenous, thus the intensity is higher in the proximity of the central axis of the beam and lower further away from the central axis. In addition, the longer the distance between the light source and the target, the more the intensity degrades.

The intensity, I , is defined as the average power, P , per unit area, A

$$I = \frac{P}{A} \quad (1)$$

and its unit is W m^{-2} . The unit area is considered perpendicular to the wave of energy. Often the light spot is circular in shape thus the area can be expressed as

$$A = \pi r^2, \quad (2)$$

where r (m) is the radius of the spot. However, the intensity unit typically used in retinal studies is photons per square micrometer per second. The conversion can be derived as

$$I = \frac{I_{\text{measured}}}{E_{\text{photon}}} = \frac{\frac{W}{m^2}}{Ws} = \frac{\text{photons}}{m^2s} = \frac{\text{photons}}{10^{12}\mu\text{m}^2s} \quad (3)$$

The photon energy can be calculated according to its wavelength

$$E = hf = \frac{hc}{\lambda}, \quad (4)$$

where h is Planck's constant ($6,626 \times 10^{-34}$ Js), f is frequency (Hz), c is speed of light ($2,99 \times 10^8$ m/s), and λ is wavelength (m). (Young & Freedman 2012.)

Intensity of the light beam can be adjusted by controlling the current driving the LED. More intensity adjustment can be obtained by using neutral density filters. The

amount of radiant power transmitted through the filter (I) can be calculated according to the fractional transmittance formula:

$$\frac{I}{I_0} = 10^{-d} \text{ or } I = I_0 \times 10^{-d}, \quad (5)$$

where I_0 is the incident intensity (W m^{-2}) and d is the optical density of the filter (m). (Horiba Scientific 2013.)

Duration

In ERG recordings, the LED light source is triggered with different kinds of pulses. These pulses can take different waveforms such as the sine wave and rectangular wave. The square and rectangle waves are used to deliver 20 ms – 2 s –step pulses for example. The sine wave on the other hand, is often used to produce flicker pulses. The frequency of the flicker has to be adjustable since different electrophysiological phenomena arise in different frequencies. For example, the separation of rod- and cone-mediated vision can be achieved with different stimulus frequencies. Flicker fusion frequency is a value used in connection with the phenomenon where the eye cannot perceive the stimulation as flicker anymore but as a continuous stimulus. (Birch 2006.)

Size

The size of the LED light beam is defined as the diameter of the spot of light. The diameter depends on the light source, the optics, and especially the mechanism that is utilized to deliver the light to the retinal sample. The most common ways to deliver the light to the sample are light guides and mirrors.

In order to make the light spot homogeneous, condenser-diffuser lenses can be utilized, for example. The condenser-diffuser lens diffracts and gathers the light thus producing uniform illumination pattern. The homogenized light beam is guided into the light guide that homogenizes the beam even further. The diameter of the light spot depends on the diameter of the light guide as well as on the degree of collimation. Additional lenses can be attached to the tip of the light guide if the light spot needs to be further modified.

Another way to guide the light to the sample is to use mirrors. When placed appropriately, mirrors can guide the light beam in an open space from the light source to the sample. Different kinds of lenses can be used to modify the beam with mirrors as well. However, the light source has to be in close vicinity of the sample due to the need of having unobstructed path for the light beam. In addition, the attenuation and scattering of the light restrict the distance between the light source and the sample. Therefore, the light guide is a more flexible solution than the mirrors.

3 RESEARCH METHODS AND MATERIALS

The practical part of the thesis is presented in this chapter. The construction of the stimulation setup starts with defining the required parameters. For clarity, the setup has been divided into two parts: the measurement setup and the light stimulation setup. Figure 3.1 presents the basic structure of the stimulation setup.

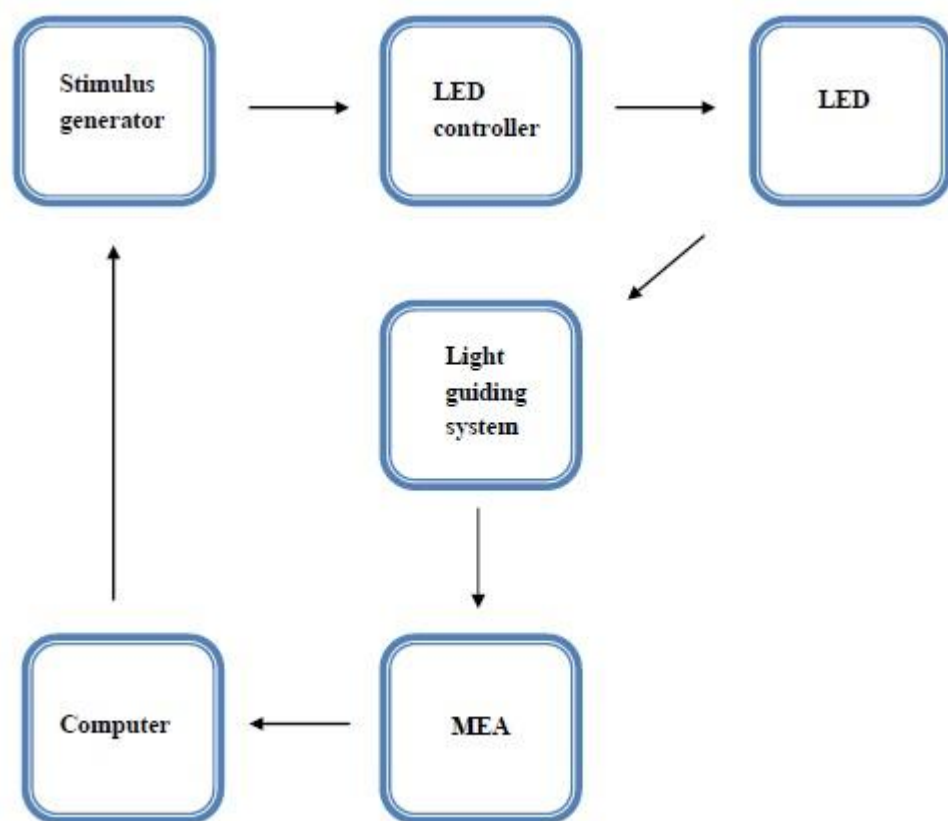


Figure 3.1. Schematic of the stimulation setup.

In this chapter, the main components of the measurement setup are presented and the structure of the stimulation setup is described. The procedure of tissue preparation is discussed in connection with the testing of the stimulation setup.

3.1 Parameter Requirements

The developed setup is intended for *in vitro* microERG recordings. It will be mainly utilized to study the ERGs of isolated mouse retinas. In order to achieve the reliable stimulation of the retinal cells, a few parameter requirements have to be met. Since the

recording of the induced responses is largely standardized with the MEA system, the main focus here is on the stimulus parameters. Meeting all the parameter requirements is crucial in order to reproduce the measurements and achieve valid results.

The peak wavelength of the stimulus is chosen to be 505 nm in accordance with the peak sensitivities of the mouse rods and one type of cones. The intensity of the stimulus pulse has to be adjustable and reliable. The intensity range has to cover approximately six decades on a logarithmic scale and it has to be linear. This ensures a sufficient intensity for both rods and cones. The required wavelength range and maximum intensity can be achieved with proper light source selection. The intensity can be adjusted by placing neutral density filters in the beam path. The filters are chosen based on the required attenuation.

The light beam has to be uniform and its diameter has to be adjustable. Here, the diameter of the stimulus spot depends on the diameter of the light guide as well as on the distance between the tip of the light guide and the retinal sample. However, possible future adjustments of the size can be taken into consideration through the possibility of attaching extra lenses to the tip of the light guide. The uniformity of the spot can be achieved by choosing appropriate lenses on the stimulus beam path.

The overall reliability of the setup and reproducibility of the measurements can be achieved by constructing a rigid setup that ensures firm placement of the components. In addition, the light source mounting is constructed so that the light sources can be easily switched in the future.

3.2 Measurement Setup

The measurement setup enables the recording, processing, and analyzing of the induced electrical responses. The setup consists of a MEA system that is controlled by a computer and is used for the recording of the responses.

Processing and analyzing the signals is done with the same computer software that is used to record the data. In addition, there are other software programs available to further analyze the signals. The components of the MEA system already existed at the time of the setup construction.

MEA System

The MEA system consists of a MEA head stage, filter amplifier, temperature controller, perfusion cannula, vacuum pump, analog-to-digital (A/D) converter, and computer. The main components of the MEA system are connected to the computer which serves as means to record the data, control the stimuli, process the data, and examine the results. In order to eliminate external interference, all the components of the MEA system are placed inside a Faraday cage, except the computer, vacuum pump, and temperature controller. In addition, the components inside the Faraday cage are separately grounded. (Multi Channel Systems MSC GmbH 2011a.)

The retinal sample is placed on the MEA that records the induced potentials. The chosen MEA type is a perforated MEA (60pMEA200/30iR-Ti). It allows the perfusion of the retinal sample from both sides at the same time, and also enables the perfusion solution to go through the retina. This ensures a good connection between the cells and the electrodes. The pMEA has 60 titanium nitride (TiN) electrodes in an 8x8 grid. The electrodes are integrated into a thin polyimide (PI) foil that is fixed on a ceramic or glass waver. The electrode diameter is 30 μm and the spacing between them is 200 μm . Figure 3.2 illustrates how the retina is placed on the MEA.

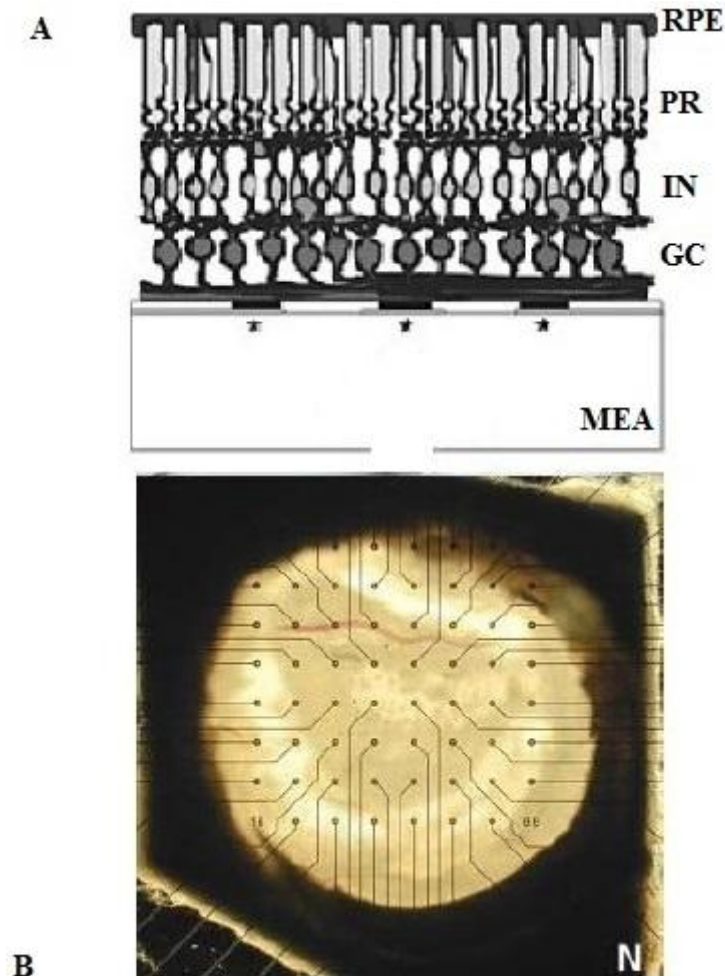


Figure 3.2. The placement of the retina on the MEA. (A) The ganglion cell layer (GC) is in contact with the electrodes. (B) A view through the MEA with the rat retina placed on it. (modified from Stett et al. 2003; Multi Channel Systems MSC GmbH 2011b)

Temperature of the retinal sample is controlled via a temperature controller unit (TC02). The retinal sample requires constant perfusion in order to stay alive and for this purpose the perfusion cannula (PH01) is attached to the MEA. This cannula is also attached to the temperature controller so that the temperature of the perfusate can be kept optimal. The perfusate is removed from the retina with a vacuum pump. (Multi Channel Systems MSC GmbH 2011a)

The recorded signal is filtered and amplified with the filter amplifier (MEA1060-Inv-BC) that is connected to the MEA head stage. The filter amplifier performs the signal filtering and amplification before it is transferred to the computer. The filter is a band pass –type with a bandwidth of 1 Hz to 3 kHz. The gain of the amplifier is 1200. (Multi Channel Systems MSC GmbH 2011a)

The recorded signal is transferred from the MEA head stage to the A/D converter that is integrated in the computer. It converts the signal from analogous to digital with the *MC_Card*-converter. The digitized signal can be graphed and analyzed with the *MC_Rack* -computer program. (Multi Channel Systems MSC GmbH 2011a)

3.3 Light Stimulation Setup

The purpose of the light stimulation setup is to produce and deliver stimuli to the retinal sample that is placed on the MEA. The light stimulation setup consists of a stimulus generator, LED controller, LED, and light guiding system. Excluding the stimulus generator, all of the aforementioned components were acquired as new.

Stimulus Generator

The stimuli used as the input of the LED are produced with the stimulus generator (STG2004) (Multi Channel Systems MSC GmbH 2011a). The generator can produce outputs from 0 V to 8 V. The output is connected to the LED controller that converts the stimuli into current form before conducting them to the LED. The stimulus generator is controlled with *MC_Stimulus II* –software that enables the modification of the stimulus waveforms and amplitudes. Complex waveforms can be produced both in current and voltage waveform. (Multi Channel Systems MSC GmbH 2011a)

LED Controller

The LED controller is a voltage-to-current converter that gets its input from the stimulus generator and conducts its output to the LED. The on- and off-time of the LED as well as its intensity is thus controlled via the stimulus generator and the LED controller. The controller that is currently used for the stimulation system can convert inputs of 0 V to 10 V into outputs of 0 mA to 20 mA. The upper limit of the stimulus generator (8 V) thus limits the output of the LED controller.

LED

The chosen light source for the stimulation is a LED from Avago Technologies (HLMP-CE13-35CDD). Its peak wavelength is 505 nm and it has a typical luminous flux of 2,1 lm at 20 mA. The forward current range of the LED is from 0 mA to 30 mA. The maximal output from the LED controller is 20 mA, so in the present system, the LED will not be driven with the full current. Figure 3.3 presents the LED behaviour in terms of relative intensity and forward current. (Avago Technologies 2010.)

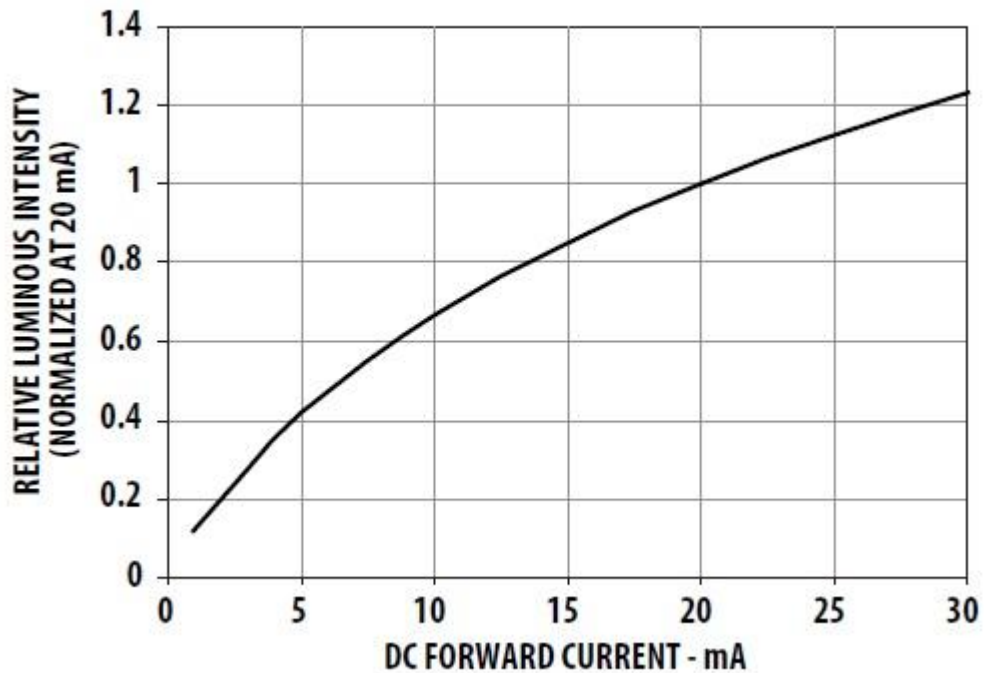


Figure 3.3. Relative intensity-forward current curve of the HLMP-CE13-35CDD LED (Avago Technologies 2010).

The LED is mounted on a Vero board that is attached to a cage plate. The cage plate is attached to the light guiding system via its construction rods. The attachment enables the fast switching of the light source if needed.

Light Guiding System

The light guiding system consists of a filter, lenses and a liquid light guide. Its purpose is to gather and transfer the filtered and collimated light from the LED to the retinal sample on the MEA. The MEA is placed on an optical breadboard inside the Faraday cage. The choice of using a liquid light guide instead of an optical fiber is due to the greater light transmission and wider light acceptance angle of the liquid light guide. (Thorlabs 2013.)

First the light from the LED is filtered with a neutral density (ND) filter. The filtered light is then gathered with a lens system that consists of two lenses: a condenser - diffuser combination lens and a condenser lens. The condenser lens with a diffuser is placed first in the beam path as it first diffuses the light rays and then aligns them on a parallel level in order to achieve a uniform illumination pattern. The second condenser lens gathers the light rays before conveying them to the liquid light guide.

The light guiding system as well as the power meter (see Chapter 3.4.1) are constructed with components manufactured by Thorlabs (Thorlabs 2013). The basis of the structure is the cage system that consists of four 60 mm construction rods (ER8) with a length of 20.3 cm. The LED is attached to the structure by mounting it on a cage plate (LCP01/M) that is attached to the construction rods. The ND filters (NE210B,

NE220B, NE230B) used in this setup have the wavelength range of 400 nm to 650 nm and their optical densities are 1,0, 2,0, and 3,0, respectively. These optical densities ensure sufficient optical attenuation. The filters are mounted on the system with a cage mount (LCP05/M). The condenser-diffuser combination (ACL5040-DG15-A) lens as well as the condenser lens (ACL5040-A) are mounted on the cage system via 60 mm cage plates (LCP06/M). The chosen liquid light guide (LLG0538-4) has a diameter of 5 mm and it is attached to the cage system with an adapter (AD5LLG). The liquid light guide adapter is attached to the cage system via a cage plate adapter (LCP02/M). Figure 3.4 presents the schematic of the light guiding system.

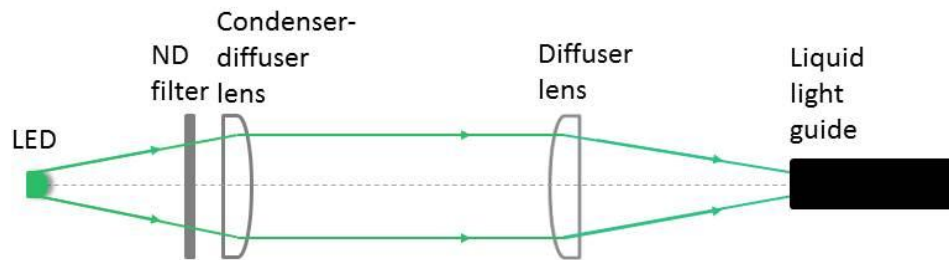


Figure 3.4. Schematic of the light guiding system.

The liquid light guide transfers the stimulus light to the retinal sample on the MEA. The MEA is placed on an optical breadboard (PBH51528) inside a Faraday cage. The position of the light guide is fixed with a pedestal post (RS4P/M) that is attached to the breadboard with a setscrew (SS6M16D). In order to position the light guide directly above the MEA, an optical post (TR150/M) is attached to the pedestal with a post clamp (RA90RS/M). The light guide is mounted on the optical post with a V-clamp (VC1/M). This enables not only the fixation of the light guide but also the adjustment of the distance between the light guide and the MEA. In addition, the light guide can be turned aside when it is not needed.

3.4 Measurement

After the light stimulation setup was put together, it had to be tested. The first part was done by calibrating the light stimulus. The purpose of this calibration was to convert the voltage values of the stimulus generator into the intensity values, and to ensure an intensity range that was linear and wide enough for ERG recordings. In addition, the ability of the stimuli to follow different waveforms was tested.

In the second part of the testing, microERGs were recorded from the isolated mouse retina. The obtained waveforms were compared to the results of other researches in order to validate them.

3.4.1 Calibration

The stimulation setup was tested and its functionality was ensured by measuring the radiant power values at the output stage. These power values were then converted into the intensity values that are crucial when studying the responses of the retinal cells to the light, in order to achieve valid results.

The calibration was done with a power meter (PM200) that measures the radiant power in relation to time (Thorlabs 2013). The power was measured at the MEA head stage level where the retinal samples are placed on. The power values were increased by adjusting the output values of the stimulus generator. These voltage steps were chosen to be 0,2 V in order to attain sufficient accuracy. The voltage range was set within the stimulus generator output range of 0 to 8 V. This range corresponds with the LED controller output range of 0 mA to *circa* 16 mA due to the very linear behaviour of the LED controller. As a result of the calibration, 40 measurement values were obtained. The measurement value of 0 V served as a reference point.

The measured values were saved in a ‘comma-separated values’ form. The data was analyzed and the power increments were detected. These increments were matched with the taken voltage steps in order to create a calibration curve that presents power in relation to voltage. The power values were then converted into intensity values with the formulas (1) and (2) that were introduced in Chapter 2.3.4.

In retinal studies, the intensity is often expressed as photons per square micrometer per second. To give the power values in these more practical units, the intensity values were converted with the formulas (3) and (4). The values needed for the formulas (1)-(4) are introduced in Chapter 3.3.

A calibration curve was created that presents the converted intensity values in relation to the voltage. In addition, the ability to follow different waveforms of the stimulus pulses was tested with sine and rectangular waves. Both waves had an amplitude of 1,0 V and they were repeated five times. The frequencies of the sine and rectangular waves were 0,16 Hz and 0,2 Hz, respectively. The frequencies of the waves were chosen according to the sampling frequency of the power meter. Since the sampling frequency was only 0,1 s, the waves had to be slow and long enough for the power meter to be able to detect them properly.

3.4.2 Tissue preparation

The final testing of the stimulation setup was done by recording microERGs from an isolated mouse retina. In order to study both rod and cone cell responses, the retinal sample had to be dark-adapted. The mouse used in the recording was kept in darkness at least three hours (preferably overnight) prior to the recording. After this dark-adaptation, the mouse was euthanized. Its eyes were quickly dissected from the animal and placed in the perfusion solution. All the procedures were performed under dim red light in order to maintain the dark-adapted state of the tissue. To isolate the retina from other tissue, the eye was hemisected and the retinal sample was gently detached from

the eye cup. The isolated retina was placed on a perfusate-lubricated filter paper that acted as a carrier for the delicate retina and allowed its placement on the MEA dish.

The retinal sample was perfused throughout the experiment with Ames' Medium (Sigma, A1420) buffered with sodium bicarbonate (NaHCO_3). This solution was bubbled with Carbogen (95% O_2 and 5% CO_2) to ensure that it was oxygenated and its pH was set to 7,4.

The isolated retina was placed on the MEA plate in the Faraday cage. The retina was placed with the ganglion cell layer facing the electrodes. The temperature of the perfusion solution was set to $37,5^\circ\text{C}$ and the vacuum pump was connected to the MEA plate for the removal of the perfusate. The vacuum of the pump was set to the desired value (here to 45 mbar) and it was placed outside the Faraday cage in order to minimize interference.

3.4.3 MicroERG Recording

Once the retinal sample was placed on the MEA and its perfusion was steady and optimal, the recording of the microERGs could be started. The recording was performed in darkness in order to obtain dark-adapted responses of the retina. First, the electrode function was ensured by recording the noise levels from them. Once the noise levels were at a tolerable level, the retina was stimulated with rectangular pulses. The pulse parameters were adjusted in terms of amplitude, duration, time between the pulses, and repetition. In addition, the light attenuation was tested with ND filters. The amplitude of the pulses was gradually increased while the pulse duration was kept constant. The time between the pulses as well as the repetition rate were altered according to the light adaptation. The used pulse parameters are listed in Table 3.4.

Table 3.4. The rectangular pulse parameters.

Amplitude (V)	Pulse duration (ms)	Time between the pulses (s)	Repetition (1)	Other
0,4	20	10	5	
0,8	20	10	5	
1,2	20	10	5	
1,6	20	10	5	
2,0	20	10	5	
2,4	20	10	5	
2,8	20	10	5	
2,8	20	20	5	
3,2	20	20	5	
3,6	20	20	5	
4,0	20	20	5	
4,0	20	20	5	ND=1,0
4,0	20	20	5	ND=2,0
4,0	20	20	5	ND=3,0
4,0	20	20	5	ND=4,0
4,4	20	30	5	

4,8	20	30	5
5,2	20	30	5
5,6	20	40	4
6,0	20	60	3
6,4	20	60	3
6,8	20	60	3
7,2	20	60	3
7,6	20	60	3
8,0	20	> 60	2

The amplitude increments of the stimulus generator were chosen to be 0,4 V. Once the amplitude of 2,8 V was reached, the time between the pulses was increased from 10 s to 20 s. Strong stimuli light-adapt the photoreceptors unless they are able to recover from the stimuli. Neutral density filters were tested with the amplitude of 4,0 V in order to ensure sufficient attenuation. The amplitude range of 4,4 V to 5,2 V was tested with 30 s between the pulses. The time between the pulses was increased to 40 s and the repetition was decreased to four times for the pulses with the amplitude of 5,6 V. The last amplitude range of 6,0 V to 7,6 V was recorded with the repetition of three times and with a time of 60 s between the pulses. The greatest amplitude of 8,0 V was recorded with two pulses, and the time between them was kept at more than 60 s to avoid light-adaptation.

4 RESULTS

The constructed setup is evaluated in three parts: the construction of the setup, calibration of the light stimuli, and measurements with retinal samples.

4.1 Construction of the Setup

The stimulation setup was constructed according to the description in Chapters 3.2 and 3.3. The measurement part of the setup consists of already existing components: the MEA head stage, filter amplifier, temperature controller, perfusion cannula, vacuum pump, A/D converter, and computer. On the other hand, all the light stimulation setup parts, except the stimulus generator, were acquired as new. Therefore, the main focus is on the stimulation part of the setup. Table 4.1 lists the utilized components.

Table 4.1. The stimulation setup components.

	Existing parts	New parts
Measurement setup	MEA head stage Filter amplifier Temperature controller Perfusion cannula Vacuum pump A/D converter Computer	
Light stimulation setup	Stimulus generator	LED LED controller Light guiding system

The construction of the light stimulation setup started with designing the light guiding system. The LED controller was not constructed by the author but it was acquired specifically for this application. The light guiding system was designed and constructed by the author. The designing of the system was based on the choice to use a LED as the light source. The choice of the LED, as discussed in Chapters 3.1 and 3.3, was based on the characteristics of a mouse retina. In addition, LEDs are easy to use, efficient, and affordable.

The frame of the light guiding system had to be rigid and stable. For this purpose, the cage system was chosen. The lenses were chosen to fit the wavelength range of the LED as well as the goal of homogenizing and collimating the light from the LED. Both lenses were chosen to have antireflective coating, focal length of 40 mm, and diameter

of 50 mm. The antireflective coating reduces the reflection and the lens diameters ensure that the lenses fit the cage system. The condenser-diffuser lens was chosen to have a finer grind (1500 Grit) due to its higher light transmittance.

The neutral density filters were chosen according to the required attenuation of the intensity. For the transmission of the light, two options were considered. Optic fibers are commonly used when light has to be transmitted from the light source to the desired target. However, liquid light guides offer better transmittance and wider light acceptance angles. This is crucial when considering the low power levels of the LED output. The liquid light guide diameter was chosen to be 5 mm in order to obtain higher light transmittance.

The light guiding system was put together by inserting the construction rods through the cage plates that held the LED, neutral density filter, lenses, and the liquid light guide adapter. The LED was placed at the end of the cage system and the filter mount was placed right after it. The condenser-diffuser lens was placed after the filter mount, before the condenser lens, in order to achieve homogenized illumination before collimating it. Finally, the liquid light guide was placed at the other end of the cage system. Figure 4.1 shows the structure of the light guiding system.

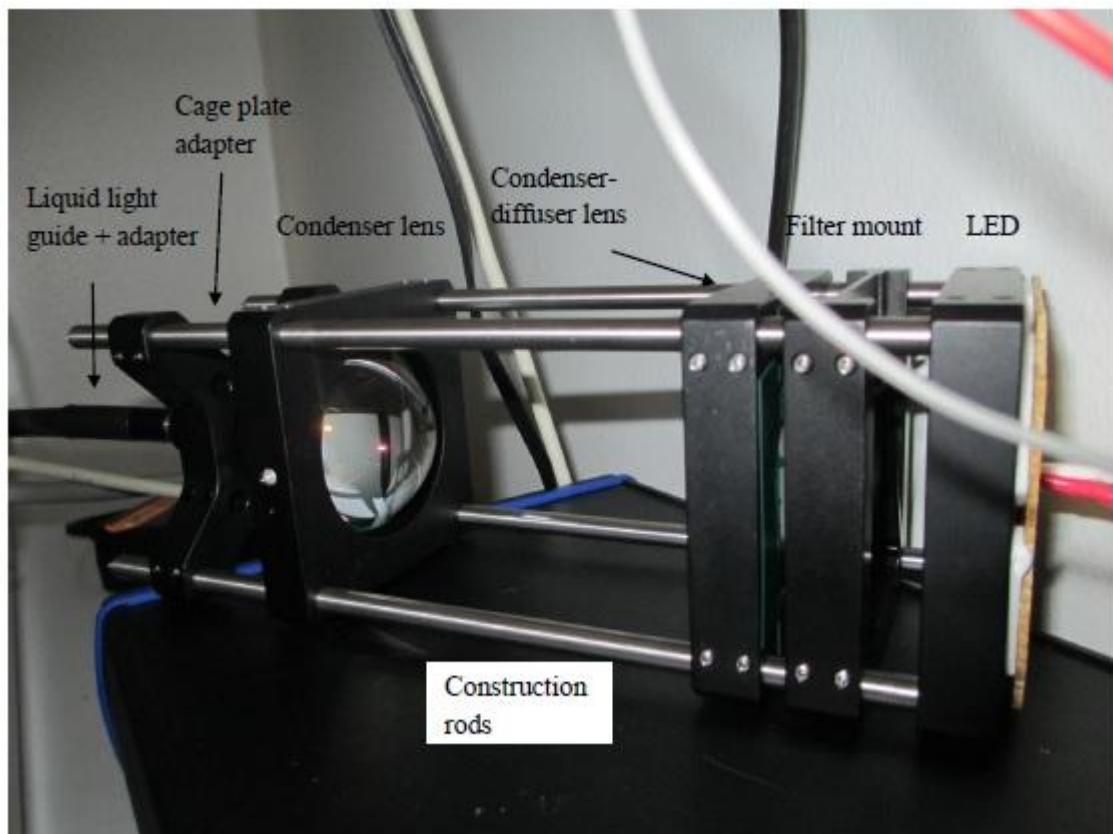


Figure 4.1. The light guiding system.

The distances between the components had to be adjusted so that the light beam could be optimized. The light beam was desired to be as homogeneous and narrow as possible. The LED and the filter mount remained stationary while the position of the

lenses and the liquid light guide was adjusted. The optimal position of the components was found by turning on the LED and searching for the optimal light beam that could be delivered to the liquid light guide.

The stimulus generator input was connected to the computer and the output was connected to the LED controller input. The LED controller output was further connected to the LED. The light from the LED was guided from the light guiding system inside the Faraday cage where only the MEA head stage, filter amplifier, and perfusion were placed. All the other parts were placed outside the cage. Figure 4.2 clarifies the setup layout.

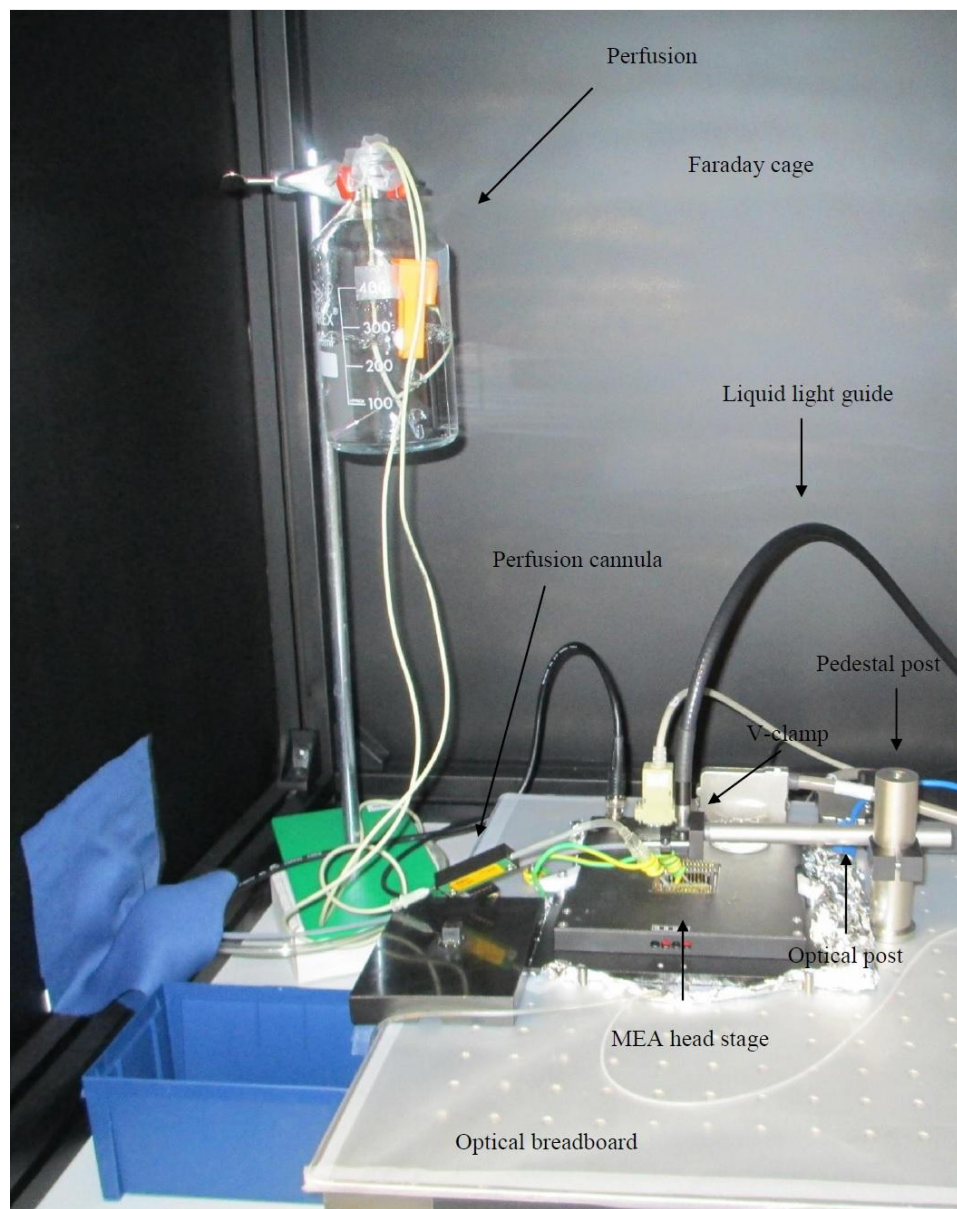


Figure 4.2. The setup layout.

The MEA head stage was connected to the filter amplifier that was further connected to the A/D converter and computer. The perfusion cannula was connected to

the temperature controller unit and to the perfusate container. The vacuum pump was attached to the MEA dish.

The MEA head stage was placed on the optical breadboard in order to minimize vibration and ensure secure placement of the light guide. In addition, damping pads were placed underneath the optical breadboard to further diminish possible vibrations. The gaps that are used as an access point to the outside components are covered with pieces of cloth in order to minimize any excess light coming from outside the Faraday cage. All the components inside the Faraday cage were grounded separately.

4.2 Light calibration

The functionality of the stimulation setup was tested by calibrating the stimulator output. Its radiant power values were measured in relation to time and the values were used to calculate the corresponding intensity values. The measured power values and the calculated intensity values are presented in the Appendix 1. For simplicity, the intensity values are presented as a magnitude of 10^8 .

Figure 4.3 presents the measured radiant power values in a power-voltage curve. The power values are presented as a magnitude of 10^{-5} for simplicity. They were matched with the stimulus generator output voltage steps of 0,2 V. The values show clear linearity throughout the whole stimulus generator output range of 0 V to 8 V. The output value of 0 V serves as a reference point.

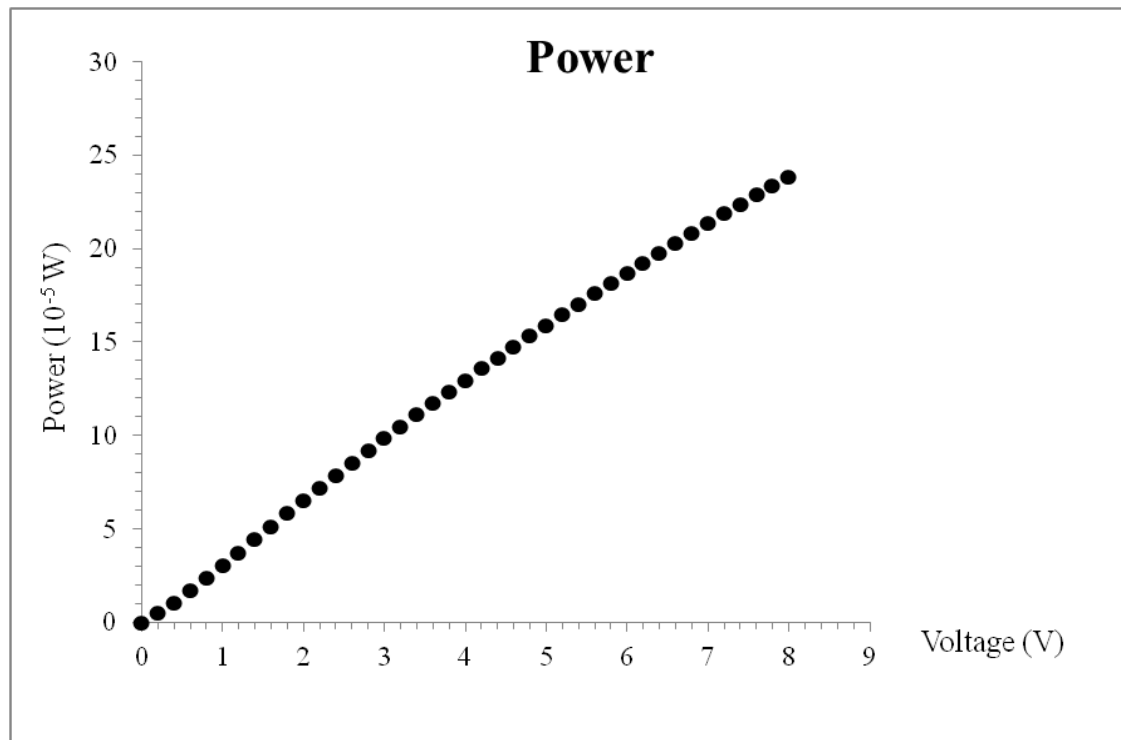


Figure 4.3. Power-voltage calibration curve.

In retinal recordings, it is often more useful to examine the stimulator output values in units of photons per square micrometer per second. This helps, for example, to determine the desirable intensity values when examining the responses of the photoreceptors. Figure 4.4 presents the calculated intensity values in an intensity-voltage curve. The curve shows clear linearity throughout the whole voltage range.

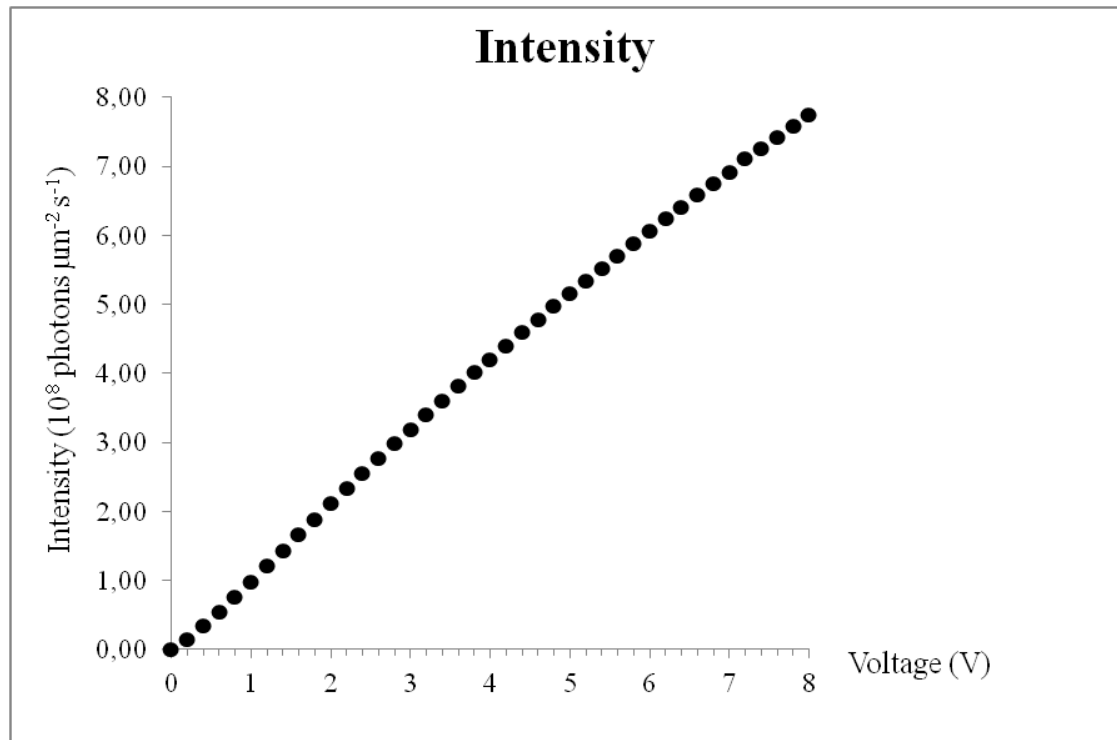


Figure 4.4. Intensity-voltage calibration curve.

The stimulator has to be able to produce low intensities. This is especially crucial when studying the responses of the rod cells. In order to determine the lowest possible intensity value, the formula (5) and the values listed in Table 4.2 are utilized. The result is also listed in Table 4.2.

Table 4.2. The lowest intensity value.

Voltage (V)	Initial intensity (W m⁻²)	Optical density	Intensity (W m⁻²)	Intensity (photons μm⁻² s⁻¹)
0,2	6,0571	5,0	6,0571×10 ⁻⁵	154,517

The lowest intensity of 154 photons per square micrometer per second indicates that intensity values suitable for the rod cells can be achieved. Thus, the whole intensity range is from 154 photons μm⁻² s⁻¹ to 7,74×10⁸ photons μm⁻² s⁻¹. This equals to an intensity range of six decades in logarithmic scale. Note however, that the lowest intensity value was calculated by using the smallest stimulus generator voltage step

taken during the measurement. Even lower intensity values can be obtained with smaller stimulus generator output values.

In addition to the linearity, the light stimulus also has to be able to produce different waveforms with different durations and frequencies. For this purpose, the radiant power of the stimulator output was measured while the stimulus generator output was set to sine- and rectangular waves. Due to the LED being a semiconductor that allows an electric current to flow in one direction, only the positive halves of the sine wave turn on the LED. Figure 4.5 presents the positive half of the obtained sine wave with a frequency of 0,16 Hz.

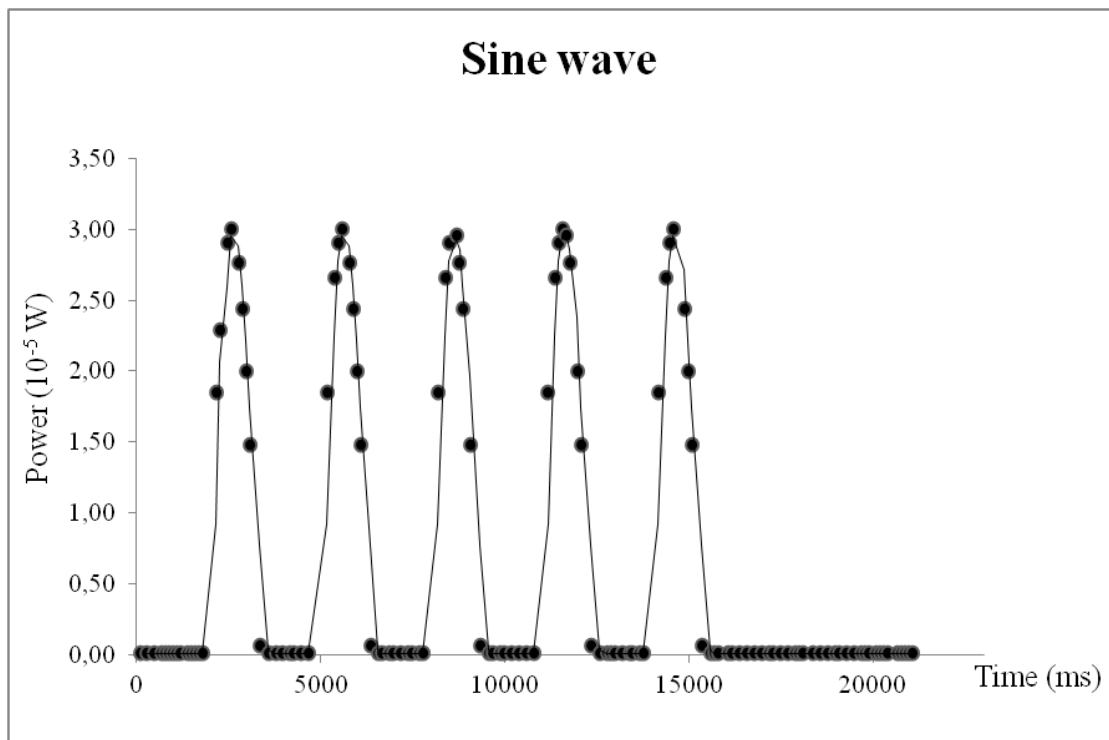


Figure 4.5. Radiant power of the stimulator output while the stimulus generator output is a sine wave.

The stimulator has to be able to produce step pulses with different durations. In order to test that, the stimulus generator output was set to produce pulses with amplitude of 1 V. The pulse frequency is 0,2 Hz with pulse duration of 3 s and the time between the pulses of 2 s. Figure 4.6 presents the recorded signal.

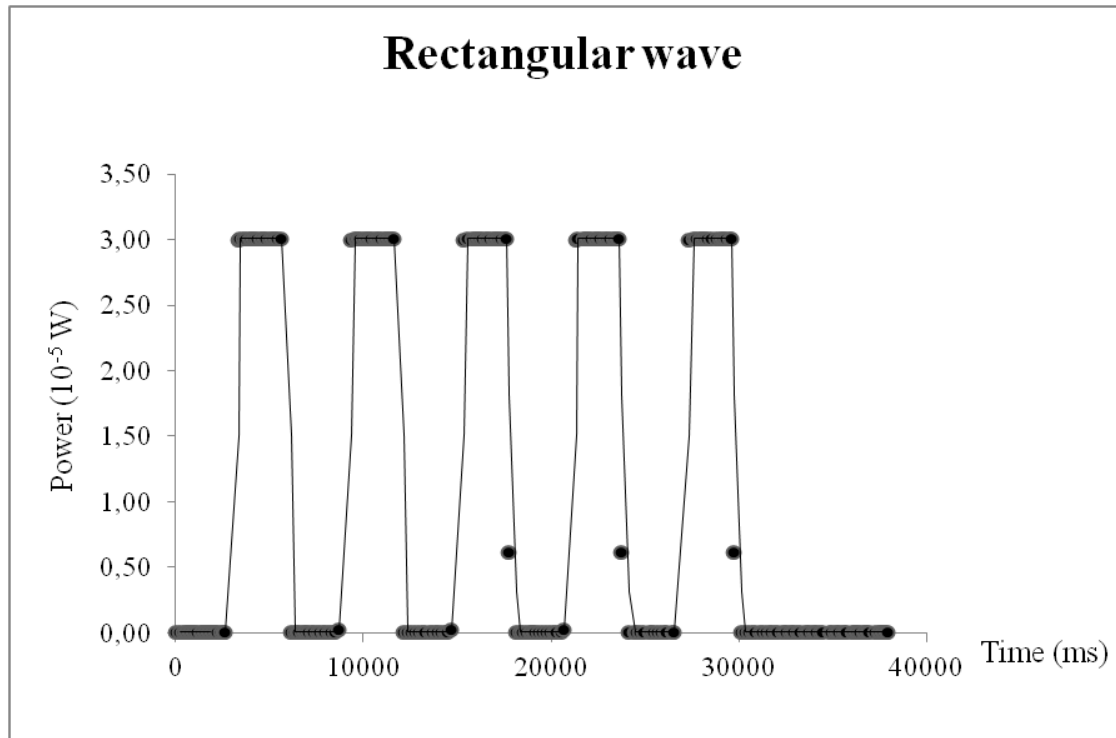


Figure 4.6. Radiant power of the stimulator output while the stimulus generator output is a rectangular wave.

The stimulator output was able to follow the stimulus generator output with both sine and rectangular waves. The frequencies of the waves were chosen according to the sampling frequency of the power meter that was 0,1 s. The power meter could not detect fast waveforms as can be seen from the distortion of the waves.

4.3 Measurements with Retinal Samples

The setup was tested by recording microERGs from isolated mouse retina. The recording was conducted according to the description in Chapter 3.4.3. Three example figures were chosen to demonstrate the obtained results. The figures present the photoreceptor responses to a 20 ms flash of light as well as the ganglion cell activity. The measurement view of the recorded channels is presented in Figure 4.7. The recorded waveforms show the photoreceptor responses as downward deflections in the signal and the ganglion cell action potentials are evident as fast spikes in several channels. The sampling frequency of the measurement was 20 kHz and the gain was 1100.

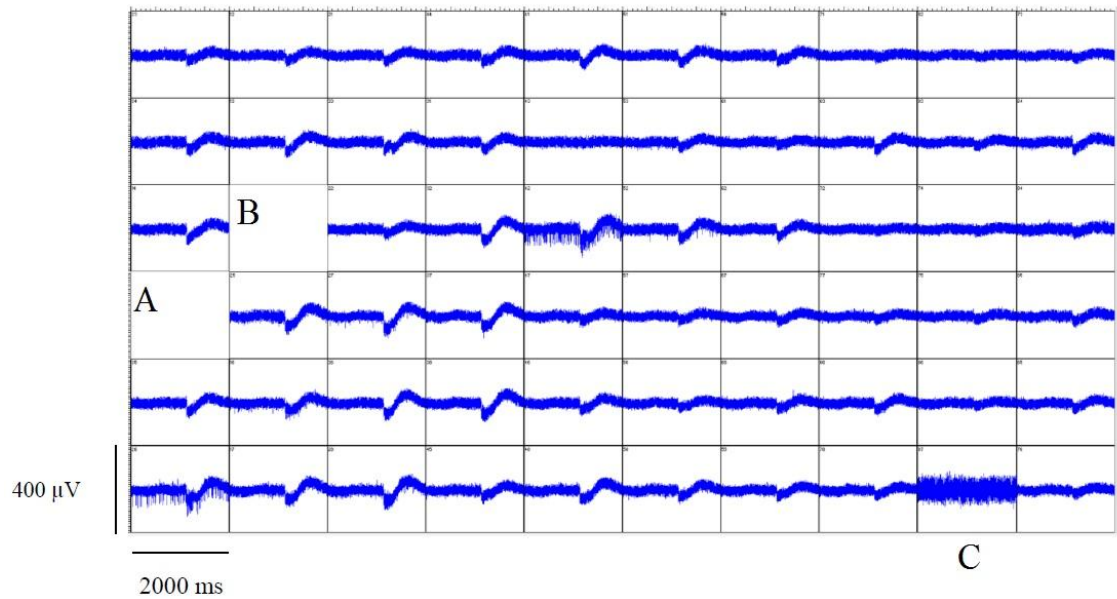


Figure 4.7. The ERG recording showing photoreceptor responses and ganglion cell action potentials. Channel (A) is the ground electrode, channel (B) is a disabled broken electrode, and channel (C) is a broken electrode.

The recorded responses were filtered in order to examine the ganglion cell activity more carefully. Two of the captured responses are presented in Figure 4.8. The upper figure (A) presents the responses of ON-OFF ganglion cells. ON-OFF ganglion cells are active in the dark. Immediately after the light stimulus, these cells produce a burst of action potentials followed by a silent period (marked as *pause* in Figure 4.8). The time of the light stimulus is shown as an arrow in the figure. The increase in the action potential firing rate evident in the figure immediately after the light pulse is the ON response and the silent period is the OFF response. The lower figure (B) presents an ON response: ON ganglion cells are quiet in the dark and their reaction to the light stimulus can be seen as a burst of action potentials right after the stimulus flash.

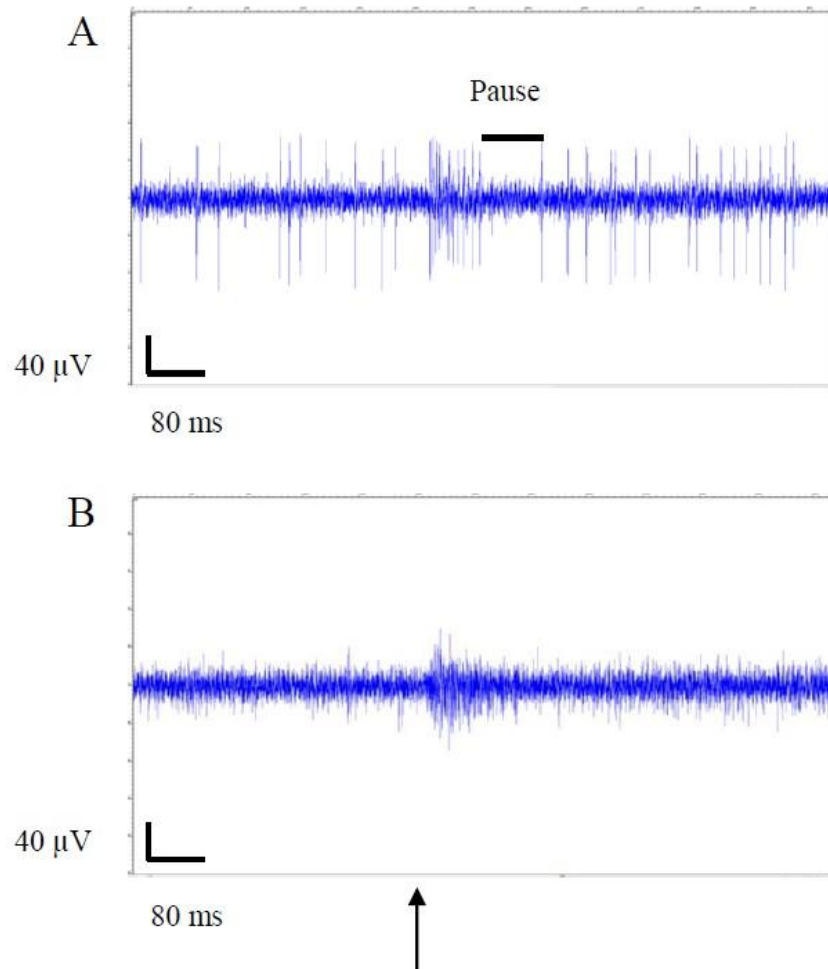


Figure 4.8. *The ganglion cell activity. The light stimulus timing is marked below the figures (arrow). (A) Presents the activity of the ON-OFF ganglion cells that fire action potentials in darkness. The increase in firing rate presents the ON response and the silent period following this burst presents the OFF response. (B) Presents the spiking of the ON ganglion cells that are silent in darkness and become active immediately after the light stimulus.*

In addition to the ganglion cell activity, the photoreceptor response was examined more closely. Figure 4.9 presents one of the recorded responses to a 20 ms flash of light.

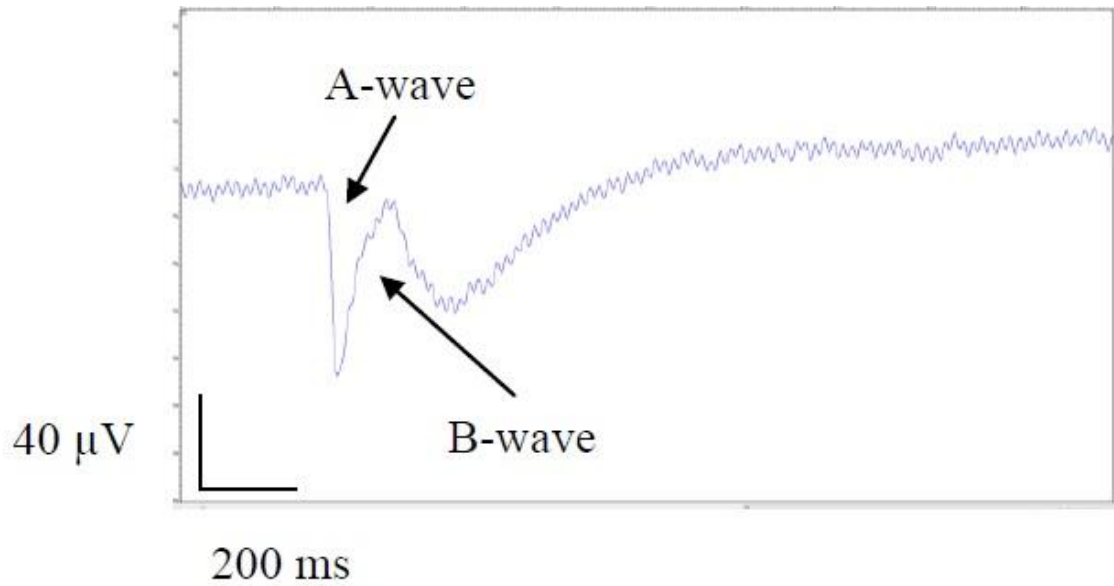


Figure 4.9. The photoreceptor response. The a- and b-waves can be clearly detected. The c-wave is absent due to the lack of the RPE. The light stimulus is applied right before the a-wave.

The photoreceptor response clearly shows the negative a-wave that is followed by the positive b-wave. The light stimulus eliciting the response is applied right before the a-wave. The c-wave is absent due to the lack of RPE.

5 DISCUSSION

The goal of this thesis was to design and construct a light stimulation setup for microERG recordings. The stimulation setup was found to be functional. The evaluation of the stimulation setup functionality can be done in three parts: the construction of the setup, stimulator output properties, and recorded microERG.

5.1 The Setup

In order to evaluate the constructed setup thoroughly, all parts of the setup are examined and evaluated separately. First, the MEA system is evaluated briefly. Then the light stimulation setup is evaluated by discussing the component choices.

The choice to use the MEA system for the microERG recordings was evident due to its ability to record both photoreceptor responses and ganglion cell activity. The MEA system is easy to use and it can provide valid results. All the components of the system were found to be functional, however, the perfusion induced noise in the recorded signals. The utilized vacuum pump did not create steady suction but it sucked the perfusate in steady intervals. This caused the perfusate level on the MEA dish to fluctuate which in turn induced the noise in the recorded signals.

The light stimulation part of the setup was mainly constructed as new. The only existing part, the stimulus generator, was tested to be functional. The LED controller was acquired specifically for the setup. The controller can convert inputs of 0 V to 10 V into outputs of 0 mA to 20 mA. The input range does not ideally correspond with the stimulus generator output range of 0 V to 8 V. Therefore, the chosen LED could not be driven with full current as its input range is from 0 mA to 20 mA.

A LED was chosen for this application because it is a small, low-cost, and easy to use light source that can produce nearly monochromatic light with high efficiency. In addition, its intensity can be adjusted and it can be turned on and off quickly. The wavelength of the LED was chosen to be 505 nm as it covers the peak absorption wavelengths of the mouse retina. Studies that utilize similar kinds of stimulation setups as the one constructed in this thesis include for example the studies conducted by Tian & Copenhagen (2003) and Herrmann et al. (2008). Both studies use LEDs as light sources. For the mouse retinas, Tian & Copenhagen (2003) used a wavelength of 567 nm and for the rat retinas, Herrmann et al. (2008) used wavelengths of 460 nm and 505 nm.

The light is guided from the LED with the light guiding system that consists of a stationary frame that supports the LED, lenses, filter, and liquid light guide as well as

the optical breadboard that minimizes any vibrations during the measurements. The chosen cage system holds the components in a steady and reliable manner. The optical breadboard provides sufficient vibration minimization during the measurements.

The neutral density filters were purchased for the setup in order to increase the stimulus intensity range. The lenses that were chosen for this setup were found to be functional, yet not ideal. Both condenser-diffuser and condenser lenses have a focal length of 40 mm. With these lenses, the beam in the inlet of the light guide was homogeneous and of optimal size. The liquid light guide was chosen over the optic fiber for the delivery of the light stimuli due to its greater light transmission. However, the light beam diffused quite strongly at the outlet of the liquid light guide. This resulted in a short distance between the MEA dish and the liquid light guide.

The construction of the light guiding system was the main responsibility of the author. The system was found to be functional, but also in a need of future improvements. The main sources of error are the aforementioned perfusion noise and the narrow space between the liquid light guide and the MEA dish. The interference caused by the vacuum pump can be solved by fixing the existing vacuum pump or replacing it with a new one that has continuous suction. Furthermore, decreasing the interference requires optimizing the suction of the pump to match with the perfusion flow that enters the MEA dish.

The narrow working space between the liquid light guide and the MEA dish makes any adjustments very challenging. In order to achieve a greater working space, a collimating lens is needed at the end of the light guide. This provides a collimated beam and enables the placement of the light guide far enough from the MEA dish.

Other studies with similar light stimulation setups such as the ones conducted by Tian & Copenhagen (2003), Herrmann et al. (2008), and Sekirnjak et al. (2009) do not present how the light is guided from the light source to the retinal sample. Therefore, comparison between the light guiding systems cannot be obtained.

The light stimulation setup constructed in this thesis fulfils the general requirements set for the light stimulation setups that are used for retinal recordings. The constructed setup can be used in microERG recordings to obtain valid results. As a conclusion, the setup can be regarded as successful.

5.2 The Stimulator Output

The stimulator output was tested with stimulus generator pulses of different magnitudes, forms, frequencies, and durations. The calibration results of the stimulator output indicated linear behavior. Figures 4.3 and 4.4 demonstrate that the power and thus the intensity range of the stimulator output can be adjusted linearly. This was an expected result based on the properties of the LED and the A/D converter. Table 4.1 indicates that the lowest intensity value is approximately $155 \text{ photons } \mu\text{m}^{-2} \text{ s}^{-1}$. As can be seen from the Appendix 1, the highest intensity value is $7,74 \times 10^8 \text{ photons } \mu\text{m}^{-2} \text{ s}^{-1}$. Thus a total intensity range of six decades in logarithmic scale was obtained.

The sufficiency of the intensity range is evaluated by comparing the obtained intensity range to values in the literature. Typical intensity range needed for isolated mouse retina recordings is approximately 4–43 000 photons μm^{-2} for rods and 2 000–2 400 000 photons μm^{-2} for cones (Heikkinen et al. 2011). By taking into account the length of the stimulus flash, the smallest intensity that can be obtained with our stimulus system is 3 photons μm^{-2} and the largest intensity is 15 480 000 photons μm^{-2} . Thus the intensity range of the stimulus system provided in this thesis is sufficient for the microERG recordings.

In addition to the linearity of the stimulator output, the stimuli can be modified in terms of duration, form, and frequency. Figures 4.5 and 4.6 show that the stimulator can produce pulses with forms of sine waves and rectangular waves. The duration and frequency of the waves can also be modified. These modification options are adequate for the present purposes.

5.3 The MicroERGs

The obtained microERG recordings show clear photoreceptor responses and ganglion cell activity. These results can be compared with studies that have utilized microelectrode arrays while recording the same responses. For example, studies conducted by Herrmann et al. (2008) and Sekirnjak et al. (2009) published the photoreceptor responses and ganglion cell activity of a rat retina, respectively. Since rat and mouse retinas are very much alike, the comparison is justified. Figure 2.8 presents the photoreceptor response and Figure 2.9 presents the ganglion cell action potentials. When comparing these with the microERG recordings obtained in this thesis (Figures 4.8 and 4.9), a clear similarity can be observed. Therefore, the obtained results are valid and the use of the setup in retinal recordings is justified.

The microERG has an important role in ophthalmic research. It provides a tool to assess the functioning of the retina as well as means to find the cause of abnormalities in the retinal signaling. Various ophthalmic studies investigate different retinal degenerative diseases, such as AMD and glaucoma, which are the leading causes of blindness worldwide. Currently, only a limited amount of treatment methods are available for these diseases. Thus, the need for retinal studies and therefore the recording of microERGs is undeniable.

6 CONCLUSIONS

In this thesis, a light stimulation setup for in vitro microERG recordings was designed, constructed, and tested. The setup will be utilized in ophthalmic research conducted in the laboratories led by Professor Jari Hyttinen, Academy of Finland Research Fellow Heli Skottman, and Academy of Finland Post-doctoral researcher Soile Nymark. The aim of this research is in understanding the functioning of the retina and RPE in health and in disease as well as in providing possible new treatment methods.

In the designed system, microERGs are recorded from isolated mouse retinas with a MEA system. The light stimulation of the retina is produced with a LED that has a wavelength that corresponds with the peak sensitivities of the mouse photoreceptors. The light from the LED is collimated and transferred to the retinal sample with a light guiding system. The system consists of a stationary frame that holds the LED, neutral density filter, homogenizing and collimating lenses, and liquid light guide.

The calibration of the light stimulator output indicated linear behaviour in terms of power and intensity levels. The intensity range is wide enough for the stimulation of the photoreceptors. In addition, the light stimulator is able to produce pulses with different magnitudes, durations, forms, and frequencies. The recorded microERGs suggest that the stimulation setup can be used to achieve valid and reproducible results.

The sources of error in the microERG recordings are the perfusion noise and the suboptimal light beam. The noncontinuous suction of the perfusate caused visible fluctuation of the ERG wave while recording. This is due to the vacuum pump which does not create steady suction but sucks the perfusion in steady intervals. The perfusion interference can be minimized by optimizing the functioning of the vacuum pump or replacing it with a more optimal one and by adjusting the perfusion flow to match better with the suction. The working space between the MEA dish holding the retinal sample and the liquid light guide can be increased if the light beam is optimized further. This would require additional lenses, especially one to be placed to the tip of the liquid light guide. When the light beam is optimal, new calibration is required.

The constructed light stimulation setup fulfils the requirements that were set for it. It can be used to stimulate the retina during microERG recordings. The objective of the thesis has been reached and thus the thesis can be regarded as successful.

REFERENCES

- Alberts, B., Johnson, A., Lewis, J., Raff, M., Roberts, K., Walter, P. Molecular biology of the cell. 5th ed. New York, USA 2008, Garland Science, Taylor & Francis Group, LLC. 1691 p.
- Avago Technologies. 2010. HLMP-CE13-35CDD. [datasheet]. [accessed on 8.4.2013]. Available at: <http://www.farnell.com/datasheets/1038179.pdf>.
- Baylor, D.A. Photoreceptor signals and vision. *Investigative Ophthalmology & Visual Science* 28(1987)1, pp. 24–49.
- Bhutto, I., & Luty, G. Understanding age-related macular degeneration (AMD): Relationships between the photoreceptor/retinal pigment epithelium/Bruch's membrane/choriocapillaris complex. *Molecular Aspects of Medicine* 33(2012)4, pp. 295–317.
- Binder, S., Stanzel, B.V., Krebs, I., & Glittenberg, C. Transplantation of the RPE in AMD. *Progress in Retinal and Eye Research* 26(2007)5, pp. 516–554.
- Birch, D.G. Flicker Electroretinography. In Heckenlively, J.R. & Arden, G.B. (eds). *Principles and Practice of Clinical Electrophysiology of Vision*. 2nd ed. Massachusetts, USA 2006, The MIT Press. pp. 581–583.
- Carr, R.E. Electroretinography. *Duane's Foundations of Clinical Ophthalmology* [electronic book]. 2006. Lippincott Williams & Wilkins. [accessed on 11.4.2013]. Available at: <http://www.oculist.net/downat0502/prof/ebook/duanes/pages/v8/v8c103.html>
- Chang, B., Hawes, N.L., Hurd, R.E., Davisson, M.T., Nusinowitz, S., Heckenlively, J. R. Retinal degeneration mutants in the mouse. *Vision Research* 42(2002)4, pp. 517–525.
- Clark, J.W.J. The Electroretinogram. In Webster, J.G. (ed). *Medical instrumentation: application and design*. 4th ed. New Jersey, USA 2010, John Wiley & Sons Inc. pp. 158–162.
- Da Cruz, L., Chen, F.K., Ahmado, A., Greenwood, J., & Coffey, P. 2007. RPE transplantation and its role in retinal disease. *Progress in Retinal and Eye Research* 26(2007)6, pp. 598–635.
- Cunha-Vaz, J.G. The blood-retinal barriers system. Basic concepts and clinical evaluation. *Experimental Eye Research* 78(2004)3, pp. 715–721.
- Ekesten, B., Gouras, P., & Moschos, M. Cone properties of the light-adapted murine ERG. *Documenta Ophthalmologica* 97(1998)1, pp. 23–31.
- Frishman, L.J. Origins of the Electroretinogram. In Heckenlively, J.R. & Arden, G.B. (eds). *Principles and Practice of Clinical Electrophysiology of Vision*. 2nd ed. Massachusetts, USA 2006, The MIT Press. pp. 139–183.

Frishman, L.J. & Wang, M.H. *Electroretinogram of Human, Monkey and Mouse*. Adler's Physiology of the Eye [electronic book]. 11th ed. 2011. Elsevier Inc.

Gerth, C. The role of the ERG in the diagnosis and treatment of Age-Related Macular Degeneration. *Documenta Ophthalmologica* 118(2009)1, pp. 63–68.

Gross, A.K., & Wensel, T.G. *Biochemical Cascade of Phototransduction*. Adler's Physiology of the Eye [electronic book]. 11th ed. 2011. Elsevier Inc.

Guenther, E., Herrmann, T., & Stett, A. 2006. The Retinasensor: An In Vitro Tool to Study Drug Effects on Retinal Signaling. In Taketani, M. & Baudry, M. (eds). *Advances in Network Electrophysiology: Using Multi-Electrode Arrays*. Springer. pp. 321–331.

Hageman, G.S., & Johnson, L.V. The Photoreceptor-Retinal Pigment Epithelium Interface. In Heckenlively, J.R. & Arden, G.B. (eds). *Principles and Practice of Clinical Electrophysiology of Vision*. 2nd ed. Massachusetts, USA 2006, The MIT Press. pp. 23–36.

Heikkinen, H., Nymark, S., & Koskelainen, A. Mouse cone photoresponses obtained with electroretinogram from the isolated retina. *Vision Research* 48(2008)2, pp. 264–272.

Heikkinen, H., Vinberg, F., Nymark, S., & Koskelainen, A. Mesopic background lights enhance dark-adapted cone ERG flash responses in the intact mouse retina: a possible role for gap junctional decoupling. *Journal of Neurophysiology* 105(2011)5, pp. 2309–2318.

Heikkinen, H., Vinberg, F., Pitkänen, M., Kommonen, B., & Koskelainen, A. Flash Responses of Mouse Rod Photoreceptors in the Isolated Retina and Corneal Electroretinogram: Comparison of Gain and Kinetics. *Visual Neuroscience* 53(2012)9, pp. 5653–5664.

Herrmann, T., Krause, T., Gerhardt, M., Hesse, M., Boven, K.-H., Stett, A. LED-based illumination system for the MEA60 system for full field stimulation of explanted retinas. *Proceedings MEA Meeting, Reutlingen, Germany, July 8-11, 2008*. Stuttgart, BIOPRO Baden-Württemberg GmbH. pp. 199-200.

Horiba Scientific. 2013. Optical Filters. [datasheet]. [accessed on 8.4.2013]. Available at: <http://www.horiba.com/uk/scientific/products/optical-filters/optical-filters-by-type/neutral-density-filters/>

International Macular Degeneration. Understanding macula degeneration. [webpage]. [accessed on 28.1.2013]. Available at: <http://www.maculardegeneration.org/agedex.html>

Kolb, H. Functional Organization of the Retina. In Heckenlively, J.R. & Arden, G.B. (eds). *Principles and Practice of Clinical Electrophysiology of Vision*. 2nd ed. Massachusetts, USA 2006, The MIT Press. pp. 47–64.

Kolb, H., Nelson, R., Fernandez, E., & Jones, B.W. Webvision-The organization of the retina and visual system [electronic book]. 2011. [accessed on 16.10.2012]. Available at: <http://webvision.med.utah.edu/>

Lukasiewicz, P.D., & Eggers, E.D. Signal Processing in the Inner Retina. Adler's Physiology of the Eye [electronic book]. 11th ed. 2011. Elsevier Inc.

MacLeish, P.R., & Makino, C.L. Photoresponses of Rods and Cones. Adler's Physiology of the Eye [electronic book]. 11th ed. 2011. Elsevier Inc.

Malmivuo, J., & Plonsey, R. Bioelectromagnetism - Principles and Applications of Bioelectric and Biomagnetic Fields [electronic book]. 1995. Oxford University Press. [accessed on 11.1.2013]. Available at: <http://www.bem.fi/book/index.htm>.

Marc, R.E. The Synaptic Organization of the Retina. Adler's Physiology of the Eye [electronic book]. 11th ed. 2011. Elsevier Inc.

Multi Channel Systems MSC GmbH. 2011a. (USB-) MEA-Systems Manual. [manual]. [accessed on 13.3.2013]. Available at: http://www.multichannelsystems.com/sites/multichannelsystems.com/files/documents/manuals/MEA-System_Manual.pdf.

Multi Channel Systems MSC GmbH. 2011b. MEA Application Note: Retina Recordings (Micro Electroretinograms) from Rattus Norvegicus. [manual]. [accessed on 15.3.2013]. Available at: http://www.multichannelsystems.com/sites/multichannelsystems.com/files/documents/applications/MEA-Applications_Retina.pdf

Naarendorp, F., Esdaille, T.M., Banden, S.M., Andrews-Labenski, J., Gross, O.P., Pugh Jr., E.N. Dark Light, Rod Saturation, and the Absolute and Incremental Sensitivity of Mouse Cone Vision. *The Journal of Neuroscience* 30(2010)37, pp. 12495–12507.

Nusinowitz, S., & Heckenlively, J.R. Evaluating Retinal Function in the Mouse Retina with the Electroretinogram. In Heckenlively, J.R. & Arden, G.B. (eds). *Principles and Practice of Clinical Electrophysiology of Vision*. 2nd ed. Massachusetts, USA 2006, The MIT Press. pp. 899–909.

Peachey, N.S., & Ball, S.L. Electrophysiological analysis of visual function in mutant mice. *Documenta Ophthalmologica* 107(2003)1, pp.13–36.

Pinto, L.H., Invergo, B., Shimomura, K., Takahashi, J.S., & Troy, J.B. Interpretation of the mouse electroretinogram. *Documenta Ophthalmologica* 115(2007)3, pp. 127–136.

Rakoczy, P.E., Yu, M.J.T., Nusinowitz, S., Chang, B., & Heckenlively, J.R. Mouse models of age-related macular degeneration. *Experimental Eye Research* 82(2006)5, pp. 741–752.

Robson, J.G., & Frishman, L.J. Dissecting the dark-adapted electroretinogram. *Documenta Ophthalmologica* 95(1999)3-4, pp. 187–215.

Robson, J.G., Maeda, H., Saszik, S.M., & Frishman, L.J. In vivo studies of signaling in rod pathways of the mouse using the electroretinogram. *Vision Research* 44(2004)28, pp. 3253–3268.

Rodieck, R.W. *The first steps in seeing*. 1st ed. Sunderland, USA 1998, Sinauer Associates Inc.

Schor, P., & Miller, D. *Optics. Adler's Physiology of the Eye* [electronic book]. 11th ed. 2011. Elsevier Inc.

Sekirnjak, C., Hulse, C., Jepson, L.H., Hottowy, P., Sher, A., Dabrowski, W., Litke, A.M., Chichilnisky, E.J. Loss of Responses to Visual But Not Electrical Stimulation in Ganglion Cells of Rats With Severe Photoreceptor Degeneration. *Journal of Neurophysiology* 102(2009)6, pp. 3260–3269.

Stett, A., Egert, U., Guenther, E., Hofmann, F., Meyer, T., Nisch, W., Haemmerle, H. Biological application of microelectrode arrays in drug discovery and basic research. *Analytical and Bioanalytical Chemistry* 377(2003)3, pp. 486–495.

Strauss, O. The Retinal Pigment Epithelium in Visual Function. *Physiological Reviews* 85(2005)3, pp. 845–881.

The Angiogenesis Foundation. *The Science of AMD*. [webpage]. [accessed on 2.4.2013]. Available at: <http://www.scienceofamd.org/learn/>

Thorlabs. *Products*. [webpage]. [accessed on 18.2.2013]. Available at: <http://www.thorlabs.de/Navigation.cfm>

Tian, N., & Copenhagen, D.R. Visual Stimulation Is Required for Refinement of ON and OFF Pathways in Postnatal Retina. *Neuron* 39(2003)1, pp. 85–96.

Wandell, B.A. *Foundations of Vision* [electronic book]. 1995. 1st ed. Sinauer Associates Inc. [accessed on 10.4.2013]. Available at: <https://www.stanford.edu/group/vista/cgi-bin/FOV/>

Wang, J.-S., & Kefalov, V.J. The Cone-specific visual cycle. *Progress in Retinal and Eye Research* 30(2011)2, pp. 115–128.

Wimmers, S., Karl, M.O., & Strauss, O. Ion channels in the RPE. *Progress in Retinal and Eye Research* 26(2007)3, pp. 263–301.

Vinores, S.A., Seo, M.S., Okamoto, N., Ash, J.D., Wawrousek, E.F., Xiao, W.-H., Hudish, T., Derevjani, N.L., Campochiaro, P.A. Experimental models of growth factor-mediated angiogenesis and blood-retinal barrier breakdown. *General Pharmacology* 35(2000)5, pp. 233–239.

World Health Organization. *Global data on visual impairments*. 2010. [webpage]. [accessed on 28.1.2013]. Available at: <http://www.who.int/blindness/GLOBALDATAFINALforweb.pdf>.

World Health Organization. Prevention of Blindness and Visual Impairment. 2013. [webpage]. [accessed on 28.1.2013]. Available at: <http://www.who.int/blindness/en/>

Young, H.D., & Freedman, R.A. University Physics. 13th ed. California, USA 2012, Addison Wesley. 1529 p.

APPENDIX 1: MEASURED RADIANT POWER VALUES AND CALCULATED INTENSITY VALUES

Table 6.1. The measured radiant power values and the calculated intensity values.

Voltage (V)	Radiant power (W)	Intensity (W m⁻²)	Intensity (10⁸ photons μm⁻² s⁻¹)
0	9,55464×10 ⁻¹⁰	0,0012166	3,10×10 ⁻⁵
0,2	4,7567×10 ⁻⁶	6,0571	1,54×10 ⁻¹
0,4	1,071260×10 ⁻⁵	13,6419	3,48×10 ⁻¹
0,6	1,7043×10 ⁻⁵	21,7025	5,53×10 ⁻¹
0,8	2,3613×10 ⁻⁵	30,0687	7,66×10 ⁻¹
1,0	3,0487×10 ⁻⁵	38,8221	9,90×10 ⁻¹
1,2	3,7405×10 ⁻⁵	47,6314	1,21
1,4	4,4353×10 ⁻⁵	56,479	1,44
1,6	5,1333×10 ⁻⁵	65,3673	1,67
1,8	5,8309×10 ⁻⁵	74,2506	1,89
2,0	6,5251×10 ⁻⁵	83,0905	2,12
2,2	7,2060×10 ⁻⁵	91,7611	2,34
2,4	7,8839×10 ⁻⁵	100,3934	2,56
2,6	8,5451×10 ⁻⁵	108,8131	2,77
2,8	9,2028×10 ⁻⁵	117,1883	2,99
3,0	9,8504×10 ⁻⁵	125,4348	3,20
3,2	10,4859×10 ⁻⁵	133,5273	3,40
3,4	11,1208×10 ⁻⁵	141,6121	3,61
3,6	11,7522×10 ⁻⁵	149,6523	3,81
3,8	12,3629×10 ⁻⁵	157,429	4,01
4,0	12,9718×10 ⁻⁵	165,1827	4,21
4,2	13,579×10 ⁻⁵	172,9148	4,41
4,4	14,1734×10 ⁻⁵	180,4838	4,60
4,6	14,7595×10 ⁻⁵	187,9472	4,79
4,8	15,3389×10 ⁻⁵	195,3253	4,98
5,0	15,9107×10 ⁻⁵	202,6066	5,16
5,2	16,4779×10 ⁻⁵	209,8293	5,35
5,4	17,0389×10 ⁻⁵	216,9731	5,53
5,6	17,5975×10 ⁻⁵	224,0863	5,71
5,8	18,1443×10 ⁻⁵	231,0492	5,89
6,0	18,6894×10 ⁻⁵	237,9905	6,07
6,2	19,2348×10 ⁻⁵	244,9356	6,24
6,4	19,7667×10 ⁻⁵	251,7089	6,42
6,6	20,294×10 ⁻⁵	258,4235	6,59
6,8	20,8178×10 ⁻⁵	265,0935	6,76
7,0	21,338×10 ⁻⁵	271,7178	6,93
7,2	21,9103×10 ⁻⁵	279,0054	7,11
7,4	22,3985×10 ⁻⁵	285,2222	7,27
7,6	22,8738×10 ⁻⁵	291,2746	7,42

7,8	$23,366 \times 10^{-5}$	297,5423	7,58
8,0	$23,8585 \times 10^{-5}$	303,8138	7,74
